Climate dynamics of a hard snowball Earth

R. T. Pierrehumbert
Department of Geophysical Sciences, University of Chicago, Chicago, Illinois, USA

Received 25 June 2004; revised 12 October 2004; accepted 12 November 2004; published XX Month 2005.

[1] The problem of deglaciating a globally ice-covered ("hard snowball") Earth is examined using a series of general circulation model simulations. The aim is to determine the amount of CO_2 that must be accumulated in the atmosphere in order to trigger deglaciation. Prior treatments of this problem have been limited to energy balance models, which are incapable of treating certain crucial physical processes that turn out to strongly affect the conditions under which deglaciation can occur. CO_2 concentrations up to .2 bars are considered in the general circulation model simulations, and even at such high CO_2 content the model radiation code is found to perform well in comparison with codes explicitly designed for high CO_2. In contrast to prevailing expectations, the hard snowball Earth is found to be nearly 30 K short of deglaciation, even at .2 bars. The very cold climates arise from a combination of the extreme seasonal and diurnal cycle, lapse rate effects, snow cover, and weak cloud effects. Several aspects of the atmospheric dynamics are examined in detail. The simulations indicate that the standard scenario, wherein snowball termination occurs after a few tenths of a bar of CO_2 has built up following cessation of weathering, is problematic. However, the climate was found to be sensitive to details of a number of parameterized physical processes, notably clouds and heat transfer through the stable boundary layer. It is not out of the question that other parameterization suites might permit deglaciation. The results should not be construed as meaning that the hard snowball state could not have occurred, but only that deglaciation requires the operation of as-yet undiscovered processes that would enhance the climate sensitivity. A brief survey of some of the possibilities is provided. *INDEX TERMS:* 0320 Atmospheric Composition and Structure: Cloud physics and chemistry; 3319 Meteorology and Atmospheric Dynamics: General circulation; 3344 Meteorology and Atmospheric Dynamics: Paleoclimatology; 5707 Planetology: Fluid Planets: Atmospheres—structure and dynamics; *KEYWORDS:* snowball Earth, Neoproterozoic, deglaciation

Citation: Pierrehumbert, R. T. (2005), Climate dynamics of a hard snowball Earth, *J. Geophys. Res.*, *110*, XXXXXX, doi:10.1029/2004JD005162.

1. Introduction

[2] The possibility that the Earth suffered episodes of global glaciation as recently as the Neoproterozoic has engaged the imagination of a considerable spectrum of the Earth Sciences community. The snowball Earth hypothesis originated with *Kirschvink* [1992]. Interest in the subject was revitalized by geological evidence reported and interpreted by *Hoffman et al.* [1998]. "Hard snowball" events, characterized by global sea ice cover, would surely number among the most consequential events of Earth's past. A review of the basic arguments favoring a hard snowball, together with a discussion of the earlier history of the idea, may be found in *Hoffman and Schrag* [2002]. Termination of a hard snowball is hypothesized to result from accumulation of a large concentration of a greenhouse gas (presumably CO_2) in the atmosphere. Many salient aspects of the snowball scenario, including deposition of cap carbonates and ^{13}C history [*Higgins and Schrag*, 2003], duration of the snowball state, and temperature of the postsnowball hothouse depend critically on the CO_2 threshold needed to trigger deglaciation. While the problem of initiation of a hard snowball has received detailed attention [*Chandler and Sohl*, 2000; *Hyde et al.*, 2000; *Poulsen et al.*, 2001; *Donnadieu et al.*, 2004; *Lewis et al.*, 2003, 2004], the estimation of the deglaciation threshold has been left to highly idealized models. In this paper, we make use of General Circulation Model simulations to develop an understanding of the nature of the climate of the hard snowball state and the way it changes as CO_2 is increased to very high concentrations.

[3] Our main interest is in clarifying the conditions necessary for deglaciation, but a better understanding of the hard snowball climate is valuable in and of itself, for addressing questions of refugia for photosynthetic life and other issues. The deglaciation problem is also of interest because, whether or not a hard snowball ever occurred on Earth, it certainly represents a crisis to which habitable planets are susceptible; knowing the circumstances in which

0148-0227/05/2004JD005162$09.00

the crisis can be surmounted therefore has implications for the occurrence of habitable planets elsewere in the universe. Finally, the hard snowball climate poses a challenge to our basic understanding of climate dynamics. It is salutary to try the mettle of the arsenal of theoretical ideas built up over the years against such a radically different climate, and see if they indeed have as much explanatory power as one would hope. The present work builds on the simulations reported in *Pierrehumbert* [2004]; the key results from the earlier work are incorporated in section 3, for the convenience of the reader.

1.1. Prior Estimates of the Deglaciation Threshold

[4] Current estimates of the CO_2 threshold required for deglaciation are based for the most part on the 1D Energy Balance Model (EBM) formulated by *Caldeira and Kasting* [1992], hereafter CK92. This model takes into account realistic CO_2 radiation physics, given certain assumptions about the vertical temperature and humidity profiles. It is assumed that clouds reduce the outgoing longwave radiation (OLR) by a fixed amount, independant of latitude and climate. The 1D EBM incorporates the qualitative effects of meridional temperature variations, but has no dynamics and therefore represents dynamical atmospheric heat transport by a meridional thermal diffusivity. The model is driven by annual mean insolation, whence the effects of seasonal temperature variations are not modeled.

[5] The deglaciation threshold of .12 bars for modern insolation, quoted from Figure 1 of CK92, is often taken as a starting point for discussions of Neoproterozoic snowball termination. However, it should be noted that this value assumes that deglaciation occurs when the annual mean equatorial surface temperature reaches 263 K, or 10 degrees below freezing. This may be a reasonable assumption for thin midlatitude sea ice which could be melted in a single summer season, but a threshold annual mean of 273 K would be more appropriate for the thick ice that would form in hard snowball conditions. For a 273 K threshold temperature, deglaciation in the CK92 model does not occur until .15 bars under modern insolation. Based on a reimplementation of the model, or less accurately measured from Figure 2 of CK92, the corresponding value for Neoproterozoic insolation is .29 bars. These results are based on an assumed surface albedo of .667 and a horizontal diffusivity of .6334 W/m^2 K. (The surface albedo .663 printed in CK92 is a misprint. Also note that the ice-free surface albedo stated in CK92 is a misprint and should be .3495 + .210 $P_2(x)$. The latter misprint does not affect the hard snowball case, but is important to note if one is trying to check a reimplementation of the model by reproducing the partially glaciated results. Note that although the surface albedo is .667, the planetary albedo is actually considerably lower in the model, since atmospheric solar absorption is taken into account.) *Tajika* [2003] finds a far lower Neoproterozoic threshold of .16 bars, because he assumes a lower surface albedo (.62) and a weaker meridional diffusivity (.455 W/m^2 K). (This is roughly consistent with Figure 2 of *Tajika* [2003], but was computed from a reimplementation of the model, owing to the difficulty of measuring an accurate value from the figure.)

[6] *Hyde et al.* [2000] computed a deglaciation threshold using a 2D geographically resolved EBM. This model evidently does not incorporate cloud effects through an OLR adjustment, but rather tunes the surface albedo to fit modern data; in consequence, it is rather difficult to say what implicit cloud effects are incorporated in the calculation. Moreover, the influence of CO_2 changes is imposed as a specified top-of-atmosphere radiative adjustment, rather being computed from a radiation model as in CK92. Because this radiative forcing in reality has to do the job of part of the water vapor feedback, as well as the solar absorption effects included in CK92 but neglected in *Hyde et al.* [2000], it is exceedingly difficult to translate the latter results into an effective CO_2 threshold. *Hyde et al.* [2000] find that, for Neoproterozoic insolation, an additional 70 W/m^2 of radiative forcing above modern values would be needed to trigger deglaciation. They suggest that this is roughly equivalent to .3 bars of CO_2, but in fact the OLR expression in CK92 indicates that about .7 bars would be needed to provide the required radiative forcing. It is possible that the high value compared to other EBM estimates arises from the neglect of cloud effects. We note in passing that *Jenkins* [2003] attempted to estimate a deglaciation threshold in a GCM by varying the solar constant; because the distribution of heating produced in this way is so different from that produced by CO_2 changes, it is even harder to reliably translate the results into a CO_2 threshold.

[7] None of the preceding EBM estimates of the Neoproterozoic deglaciation threshold can be considered as definitive, because of the inherent uncertainties in estimating the parameters that go into an EBM. Four climatic characteristics crucially affect deglaciation, but are exceedingly difficult to estimate in simplified models. They are: temperature lapse rate, dynamical heat transport, snow cover, and cloud effects. Lapse rate, governed by a complex interplay of dynamics and convection, is crucial to the greenhouse effect, which can operate only insofar as the air aloft is significantly colder than the ground. Horizontal heat transport by atmospheric motions determines the extent to which the warm areas, which are the first to deglaciate, must give up some of their energy to the colder parts of the planet. An indication of the sensitivity of EBM results to the assumed meridional diffusivity can be found in *Ikeda and Tajika* [1999]. Snow cover, determined by long range transports of moisture in the atmosphere, affects the surface albedo, because snow is more reflective than sea ice [*Warren et al.*, 2002].

[8] Clouds are problematic for all modeling studies, and continue to be a primary source of uncertainty even in modern climates where we have a wealth of direct observations [*IPCC*, 2001]. Clouds are particularly important in the deglaciation problem because a high cloud over ice or snow reflects little more sunlight than the underlying surface, but provides a powerful warming effect through trapping of infrared radiation. To some extent the cloud treatment in CK92 reproduces this effect, since it is assumed that clouds reduce the OLR by a fixed 15.56 W/m^2 while the surface albedo is recomputed over icy surfaces assuming clear sky conditions. The cloud OLR adjustment adopted in CK92 is obtained by tuning the value so as to make the model fit the present mean temperature, and therefore must do the job of correcting for all model inaccuracies. Based on calculations with the ERBE data set [*Ramanathan et al.*,

1989], the observed global annual mean OLR reduction due to clouds is 29.52 W/m^2, or roughly twice the value assumed in CK92, and therefore the particular choice of cloud adjustment in CK92 must be regarded as somewhat arbitrary in the context of deglaciation. To illustrate the sensitivity to the cloud adjustment, we recomputed the results of CK92 with alternate cloud assumptions. For Neoproterozoic insolation, the model deglaciates at .53 bars if the cloud adjustment is set to zero, or .14 bars if the adjustment is fixed at its true modern value (certainly an overestimate of cloud forcing for cold glacial conditions).

[9] A simplified energy balance model with a more physically based treatment of cloud radiative forcing does confirm that there are reasonable settings of the cloud parameters that allow the deglaciation to occur at .2 bars or less in Neoproterozoic conditions [*Pierrehumbert*, 2002]. However, modest changes in the choice of cloud optical properties can push the deglaciation threshold to much higher values. It should also be noted that the estimates in *Pierrehumbert* [2002] were carried out assuming a surface albedo of .65, which is reasonable for glacier ice and some types of sea ice, but which does not account for the brightening effect of snow.

[10] Although water vapor plays a lesser role in very cold climates than it does in the modern climate, it has a not insignificant affect on the deglaciation threshold, which compounds the uncertainty of EBM estimates. In an EBM the relative humidity must generally be fixed by fiat, whereas the true relative humidity of the atmosphere is determined by dynamics and microphysics. CK92 assumed that the atmosphere was completely saturated with water vapor, leading to an overestimate of solar absorption and an under estimate of OLR, and biasing the results towards deglaciation. This was a reasonable assumption in the context of the main purpose of CK92, which was to demonstrate the extreme difficulty of deglaciating a hard snowball early in Earth's history. If one is interested in an accurate Neoproterozoic threshold, however, some reduction in the assumed relative humidity is in order, though it is difficult to say how much without help from a dynamical model.

1.2. Plan of the Paper

[11] The results of general circulation models (GCMs) should not be taken uncritically as truth, any more than should the results of EBMs. GCMs have the advantage that they rest on physics that is closer to first principles, and therefore provide a better basis for understanding mechanisms; it is in this spirit that the results of the present paper are offered. The design of the GCM experiments is described in section 2. An analysis of the thermal structure of the simulated atmosphere and its sensitivity to increase in CO_2 is presented in section 3. As the climates we find are very cold and surprisingly resistant to deglaciation, the analysis goes into some detail concerning the aspects of the radiation budget that account for the low sensitivity. Heat transport by transient eddies in storm tracks is taken up in section 4. A description of the simulated Hadley circulation is given in section 5. The behavior of the Hadley circulation raises many intriguing dynamical questions, which will be treated in a companion paper (R. T. Pierrehumbert, manuscript in preparation, 2005); in the present work we confine ourselves to a few descriptive remarks regarding the strength of the circulation and its effect on tropical temperature patterns. A brief discussion of the hydrological cycle and surface energy budget is taken up in section 6, in which we shall be primarily concerned with processes determining snow cover, and also those which produce a strong temperature inversion at the surface and help to keep the ice surface cold. Some additional experiments probing sensitivity to surface albedo and cloud assumptions are described in section 7. A general appraisal of the prospects for deglaciation of a hard snowball, in light of what has been learned from the simulations, is given in section 8.

[12] Whereas EBM results have led to the general impression that the Neoproterozoic snowball should be at least close to deglaciation at .2 bars, the GCM simulations remain far short of deglaciation even at this highly elevated CO_2 concentration. The reasons for the very cold climate rest on quite fundamental physics concerning convection, lapse rate and water vapor, and the climate is very cold despite conservative assumptions about surface albedo which should in principle favor deglaciation. More speculative assumptions permitting further lowering of the albedo of the frozen surface have been examined, and while they can lead to substantial summer midlatitude warming, they still leave the annual mean tropical ice temperature far below freezing. Alteration of the cloud assumptions so as to yield a radically increased cloud greenhouse effect produce a similar pattern of warming. The present series of simulations, however, does not come at all close to exploring the full range of possible behaviors under alternate assumptions. The factors that lead to a low tropopause in the summer hemisphere and a weak lapse rate in the winter hemisphere are not entirely straightforward. They depend to some extent on suppression of heat transfer through the stable nocturnal boundary layer, the thermal inertia of the frozen surface, solar absorption in the atmosphere and possibly resolution-dependant aspects of dynamical heat transport.

[13] Our present simulation technology cannot reliably go beyond .2 bars, and the possibility of deglaciation at 1 or 2 bars cannot be ruled out. Even at such high levels, deglaciation is expected only if new physics enters the problem in such a way as to greatly increase the climate sensitivity. It remains to be seen whether the accumulation of so much CO_2 in the atmosphere is geologically plausible, or if it would be compatible with the geochemical record attributed to the postdeglaciation climate.

[14] As with any controversial idea, the snowball hypothesis has tended to divide the community into prosnowball and antisnowball camps, much as was the case for the more sweeping revision of conventional geological thinking called for by the hypothesis of continental drift. The present work does not belong to any camp. In dealing with a time as deep in the past as the Neoproterozoic, all possible constraints must be brought to bear on the problem. No single piece of geological evidence will ever be conclusive. For example, the interpretation of the Neoproterozoic ^{13}C signal has turned out to be remarkably intricate, and not simply linked to an abiotic ocean [*Higgins and Schrag*, 2003; *Jiang et al.*, 2003]. Similarly, no simulation is likely to definitively rule out the possibility of the snowball scenario, given

uncertainties in modeling assumptions, particularly concerning cloud effects and surface albedos. Our primary goal in the present work is to extract from general circulation simulations a credible appraisal of the conditions necessary for the Earth to recover from global glaciation in Neoproterozoic conditions. By combining ever-improving model constraints with ever-improving data, one hopes eventually to arrive at some approximation to the truth. Though our results show that deglaciating a hard snowball is a much more difficult hurdle to overcome than has been generally recognized, it would be premature to infer that the hypothesis is on that account any less plausible.

2. Simulation Methods

[15] Our treatment of the general circulation of a hard snowball Earth and its implications for deglaciation is based on a series of simulations with the FOAM 1.5 GCM [*Jacob*, 1997; *Poulsen et al.*, 2001]. The version used in the present simulations is run coupled to the Semtner 3-layer thermodynamic snow/ice model [*Semtner*, 1976]. Once sea ice has built up to sufficient thickness, ocean dynamics has little effect. Hence, the simulations were carried out with a mixed-layer ocean without imposed horizontal oceanic heat transport. Run in this mode, FOAM is essentially a portable Beowulf-oriented reimplementation of CCM3 [*Kiehl et al.*, 1998], run at R15 horizontal resolution R15 ($4.5^\circ \times 7.5^\circ$) with 18 levels. The solar luminosity was set at 94% of its present value, and the paleogeography consists of an idealized equatorial supercontinent as in *Poulsen et al.* [2001] and *Jenkins* [2003]. Orbital parameters were left at the Earth's present values; we do not consider the effect of extreme obliquity variations, such as those contemplated in *Williams et al.* [1998]. The model was first run at 100 ppm CO_2 until the ocean became globally covered by sea ice of thickness of at least 5 meters. Then, a sequence of 20-year simulations was carried out, with CO_2 concentration set at 400 ppm, 1600 ppm, 12800 ppm, 10% (.1 bar) and 20% (.2 bar). Given the low thermal inertia of the ice/land surface, 20 years was found to be adequate for the climate to come into equilbrium with each CO_2 concentration. Results presented in the following are taken from the last 10 years of each run. The only quantities that fail to reach equilibrium are the ice thickness and snow depth but in neither case does the disequilibrium affect the climate; the ice becomes thick enough to insulate the atmosphere from the ocean's heat content, and the snow becomes deep enough for the snow albedo to saturate at its maximum value. Snow continues to accumulate at up to .5 cm/year of liquid water equivalent, but since surface albedo saturates at a snow depth of only .5 cm over ice, the surface albedo has ample time to equilibrate in regions of net accumulation. To assure that the ice/snow model retains adequate vertical resolution to treat the diurnal and seasonal cycle, ice thickness is clamped at a maximum of 20 m, and snow thickness at a maximum of 1 m (liquid water equivalent). This value is reached quickly, and given the low thermal diffusivity of ice is sufficient to almost completely insulate the atmosphere from the heat content of the ocean. If allowed to grow, ice thickness would continue to increase at a rate of 20–50 cm/year, further reducing the already small leakage of heat through the ice; the leakage through 20 m of ice causes the climate to be very slightly warmer than it would be if ice were allowed to reach its full thickness.

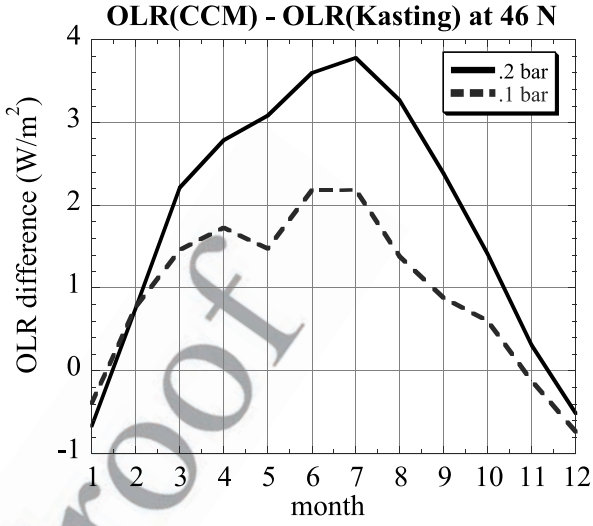

Figure 1. Comparison of OLR computed with the CCM3 radiation code used in the GCM experiments, and the more accurate Kasting-Ackerman code [*Kasting and Ackerman*, 1986]. The time series of the difference of the two models based on temperature and humidity profiles at 46N latitude, 0° longitude is shown for a single year. Positive values indicate an overestimate of OLR by the CCM3 model, relative to the Kasting-Ackerman code. Results are shown for the simulations with .1bar and .2bar of CO_2.

[16] Surface albedo is a matter that requires very serious attention, and in many respects lies at the very heart of the deglaciation problem. The snow albedo assumed in the model saturates at .9 in the visible and .60 for the near-IR when the snow is sufficiently deep, and is somewhat lower than the measured values for new snow [*Warren et al.*, 2002]; the corresponding broadband albedo based on the unmodified solar spectrum is .75. The albedo of bare sea ice was taken to be .5 independant of wavelength. This is consistent with the mean albedo for bare nonmelting ice reported in *Warren et al.* [2002], but the measurements indicate that it would be more accurate to have the albedo be somewhat higher in the visible and somewhat lower in the near-IR. Experiments with a more realistic wavelength dependance show only a weak effect (see section 7).

[17] These assumed albedos represent only a base case for building a general understanding of the problem. In reality, there are many different possibilities for the kinds of frozen surfaces that might occur on a snowball Earth, and each has its own characteristic albedo. In particular, the assumed bare-ice albedo may be unrealistically low in the tropics. The tropical region is likely to be covered by sea-glacier ice rather than sea ice, owing to flow of floating thick ice sheets from regions of net snow and ice accumulation [*Goodman and Pierrehumbert*, 2003]. For sea glaciers, an albedo of .6 would be more appropriate, based on measurements of blue glacier ice [*Warren et al.*, 2002]. The base case represents a choice that is relatively favorable to deglaciation, in that it assumes that sea glaciers for some reason do not flow rapidly enough to fill the tropics with bright sea-glacier

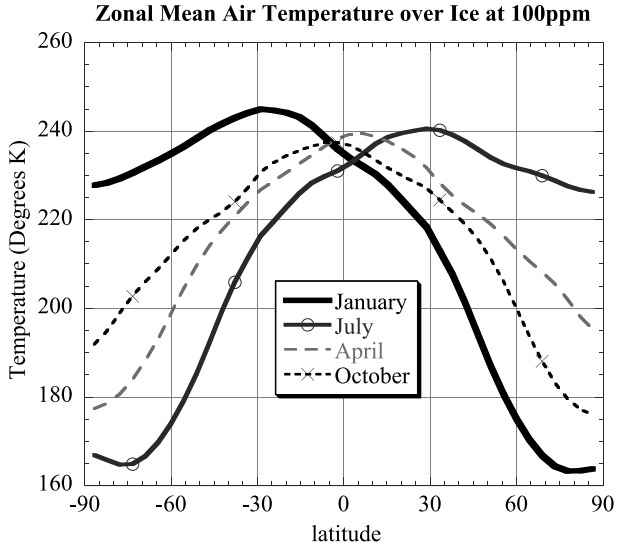

Figure 2. Seasonal cycle of zonal mean air temperature for the 100 ppm case. The temperature shown is that of the lowest model level, averaged excluding points over land.

ice. A selection of alternate albedo scenarios is discussed in section 7.

[18] The radiation module of FOAM is the same as that used in CCM3 [*Kiehl et al.*, 1998]; while 1600 ppm is well within the range for which the radiation code is validated and commonly used, there is little published basis on which to estimate the errors for CO_2 levels as high as .1 bar. To address this issue, we used a radiation model valid at high CO_2 [*Kasting and Ackerman*, 1986] to recompute the outgoing longwave radiation (OLR) corresponding to a representative sampling of the temperature and humidity profiles produced by the GCM. The accurate OLR was then compared with the OLR produced by the GCM's internal radiation code. A typical comparison is shown in Figure 1. The CCM3 radiation code overestimates the correct OLR by at worst 2.2 W/m^2 in the .1 bar case, and 3.8 W/m^2 in the .2 bar case. The simulated climate is thus very slightly colder than it should be, but the effect is inconsequential in the face of the substantial additional warming that would be needed to deglaciate, and of likely uncertainties in cloud effects and surface albedo.

3. Thermal Structure and the Greenhouse Effect

[19] The climate of the hard snowball Earth is governed by the low thermal inertia of the globally solid surface, which has the consequence that the temperature reponds primarily to the instantaneous solar radiation. The summer hemisphere becomes nearly isothermal whereas the weakly illuminated winter hemisphere becomes extraordinarily cold, resulting in an extreme seasonal cycle resembling that of Mars. The analogy with Martian climate was first made explicit by *Walker* [2001], on the basis of EBM simulations. Strong seasonality is also a well known feature from GCM simulations of the hard snowball state [e.g., *Jenkins*, 2003]. Consider the January zonal mean near-surface air temperature for 100 ppm CO_2, shown in Figure 2. The south (summer) polar temperature is 228 K, only about 17 K cooler than the subtropical temperature maximum, while the north (winter) polar temperature falls to 163 K. In July, the pattern is much the same, except reflected about the equator, yielding a 64 K high-latitude seasonal cycle. The July subtropical maximum temperature is somewhat less than the January maximum because of asymmetries of the solar heating associated with the Milankovic orbital parameters of the simulation; these result in about 30 W/m^2 difference in the maximum subtropical insolation between January and July. During the equinoxes the temperature maximum is near the equator and somewhat cooler than the January subtropical maximum. The equinox temperature pattern is approximately symmetric about the equator, but shows some asymmetry between April and October, primarily because the chosen months are somewhat past the exact equinox, and high latitude insolation varies rapidly at this time of year.

[20] For the most part, the detailed discussion in the remainder of this paper will be focused on the January near-solstice conditions. The warmest temperatures occur at this time, and these are important for determining the occurrence of seasonal surface melt pools. However, slightly below the ice surface, the temperature is determined primarily by annual mean surface conditions, and so the annual average temperature would be the most relevant statistic for determining the onset of sustained melting. Because of the extreme seasonal cycle, though, the annual average provides a poor basis for understanding the physical basis of the behavior of the climate, whereas the solstice well illustrates the range of relevant processes. The July conditions are nearly symmetric with the January ones and the equinox extratropics resemble a less extreme form of winter conditions; these cases therefore do not, in general, merit a separate discussion. Once we have built some understanding of the behavior of the climate, we will return at the end to a discussion of annual mean.

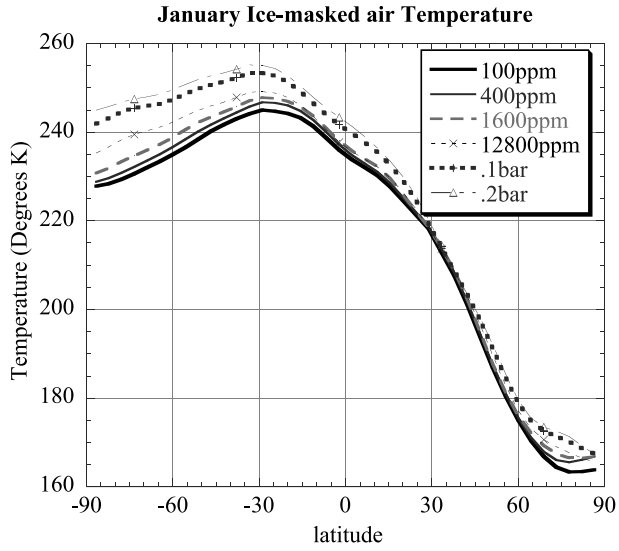

Figure 3. January zonal-mean air temperature at the lowest model level, for various CO_2. Only sea-ice grid points are used in computing the mean, so as to focus on the temperature most relevant for determining deglaciation.

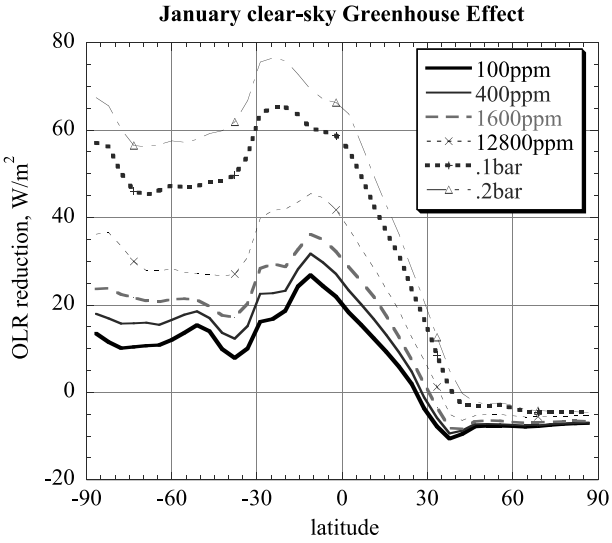

Figure 4. January zonal-mean clear-sky greenhouse trapping, for various CO_2.

[21] Figure 3 shows how the temperature changes as CO_2 is increased. The temperature in the winter hemisphere changes very little, and the maximum summer hemisphere temperature remains well short of the melting point even at .2 bars of CO_2. Even confining attention to the summer hemisphere, the sensitivity of climate to CO_2 is considerably less than would be expected from simulations under modern conditions. In the range 100 ppm to 1600 ppm, each quadrupling of CO_2 results in a tropical temperature increase of about 2 K, which is about half the sensitivity of FOAM under modern conditions, or equivalently about half the midrange sensitivity of the suite of IPCC models. At very high CO_2 levels, the sensitivity does begin to increase: the doubling between .1 bar and .2 bars brings a 2 K tropical warming.

[22] Why is the warming so weak? Figure 4 shows the diagnosed clear-sky greenhouse effect, defined as

$$G = \sigma T_s^4 - OLR_{clear} \tag{1}$$

where T_s is the surface temperature. It is actually negative in the winter extratropics, and grows only to modest values in the winter tropics. The reason for this behavior is to be found in the vertical profile of temperature, shown in Figure 5. In the winter hemisphere, the atmosphere is nearly isothermal. An examination of the convection diagnostics revealed that convection is entirely suppressed in the winter hemisphere; without convection, the atmosphere relaxes to radiative equilibrium, with a temperature inversion at the surface. Without colder air aloft, the winter hemisphere acts somewhat like the present-day stratosphere, which experiences a radiative cooling tendency in response to elevation of the CO_2 concentration. A similar situation sometimes occurs in the Antarctic winter today (see Figure 12d of *Hanel et al.* [1972]). In the summer hemisphere, convection is active but the low tropopause limits the vertical temperature constrast, in turn limiting the greenhouse effect. The greenhouse effect is limited further by the virtual lack of water vapor feedback at such cold temperatures. As a result, at .2 bars the greenhouse trapping never attains even the 100 W/m^2 typical of the present low CO_2 climate.

[23] It is not self-evident that convection should be suppressed in the winter. Certainly, the lack of a warm ocean and the weak solar heating occasioned by short days and the high-albedo surface deprives the system of much of the energy needed to sustain convection, but the story does not end there. The weak driving implies that only weak countervailing effects are needed to suppress convection, but in the absence of such effects the atmosphere would always cool down to the point where convection would start, no matter how cold the equilibrium surface temperature may be. An isolated radiative-convective atmosphere driven by steady, weak solar forcing to which the atmosphere is transparent would reach an equilibrium state having a convective tropospheric layer, no matter how small the solar flux is made. (In fact, the tropopause height in such a system will generally be only weakly dependent on the solar forcing. As a simple example, consider a dry atmosphere which is optically thin in the infrared and which has surface temperature T_s. The stratosphere will be isothermal with temperature equal to the skin temperature $2^{-\frac{1}{4}}T_s$. On the dry adiabat, the temperature decreases like $T_s(p/p_s)^{R/C_p}$, where p_s is the surface pressure. Hence the tropopause, where the adiabat intersects the stratospheric temperature, is at $p = 2^{-\frac{C_p}{4R}}p_s$, independent of temperature. In the optically thick limit, the temperature dependence of absorption coefficients will introduce a weak dependance of tropopause height on temperature.) Several factors help to suppress convection in the hard snowball winter. The high albedo surface implies that a greater portion of the net solar absorption occurs in the atmosphere rather than at the surface, reducing the rate of buoyancy generation. Dynamic transport of heat from the summer hemisphere, in the form

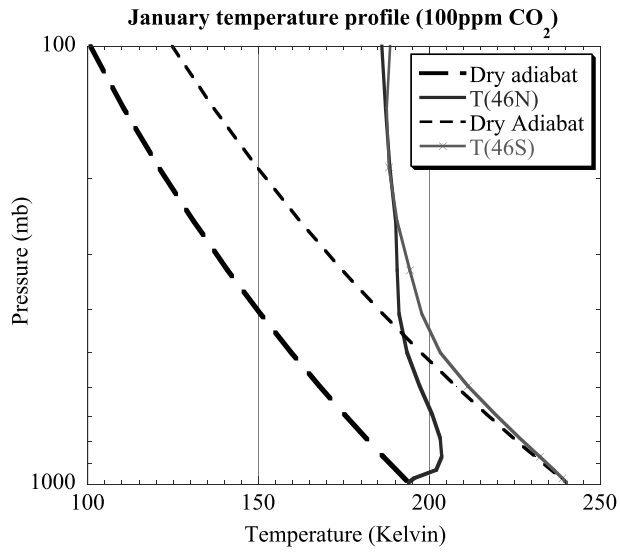

Figure 5. Typical vertical temperature profiles for the 100 ppm CO_2 case. For reference, the dry adiabat (virtually identical to the moist adiabat at these temperatures) is shown. Convection resets the temperature to the adiabat, so by comparing the actual curves with the adiabat, one can identify the layer in which convection causes the familiar sharp drop of temperature with height.

of synoptic eddy heat flux and dynamically driven subsidence, further warms the atmosphere relative to the surface. Finally, the strong diurnal cycle, to be discussed in section 6 results in a very cold stable nocturnal boundary layer, which does not warm sufficiently during the brief daylight hours to initiate convection.

[24] A further complicating factor is that the midlatitude lapse rate and tropopause are at least partly determined by synoptic eddy dynamics [*Schneider*, 2005]. This applies to the summer thermal structure as well as the winter. The subtlety of the processes involved leads one to suspect that the precise magnitude of the suppression of the greenhouse effect may be model-dependant, both through parameterization assumptions and through resolution effects which may influence synoptic eddy dynamics. Parameterization of the stable nocturnal boundary layer is apt to be particularly significant. The details of the convection scheme are unlikely to be important in the winter hemisphere, where convection is never activated. The convection parameterization may affect the summer thermal structure, but it should be recognized that there is so little moisture in the system that the convection is predominantly dry, whence the more sophisticated aspects of most convective schemes are never engaged.

[25] The greenhouse diagnostic defined in equation (1) provides a convenient indication of the net effect of the atmosphere on surface temperature, but it is not a good basis for understanding the radiative forcing changes that drive the temperature change. To understand these forcings, one can use an offline radiation code to dissect the changes in OLR between one case and another into components caused by various factors in isolation (temperature, humidity, CO_2, etc.). We adopt the formulation of *Held and Soden* [2000], and for the purposes of computing feedbacks treat the entire temperature and humidity profile as if it were a function of a single reference temperature T_a, which we take to be the air temperature at the lowest model level. The subsequent discussion will be restricted to clear sky conditions. The change in OLR between two cases with differing CO_2 may be written:

$$\Delta OLR = \gamma_T \Delta T_a + \gamma_w \Delta T_a + \gamma_{CO_2} \Delta \log_2 (pCO_2) \tag{2}$$

where

$$\gamma_T = \frac{OLR\left(T_2, q_1, (pCO_2)_1\right) - OLR\left(T_1, q_1, (pCO_2)_1\right)}{\Delta T_a} \tag{3}$$

$$\gamma_w = \frac{OLR\left(T_1, q_2, (pCO_2)_1\right) - OLR\left(T_1, q_1, (pCO_2)_1\right)}{\Delta T_a} \tag{4}$$

$$\gamma_{CO_2} = \frac{OLR\left(T_1, q_1, (pCO_2)_2\right) - OLR\left(T_1, q_1, (pCO_2)_1\right)}{\Delta \log_2 (pCO_2)} \tag{5}$$

In these formulae, T_j and q_j stand for the the full temperature and humidity profiles of the cases, and not just their values at some particular point. γ_T gives the change in OLR due to changing temperature with fixed atmospheric composition, and measures how much temperature must increase (in the absence of feedbacks) to offset a reduction in OLR caused by an increase in CO_2. γ_w characterizes the water vapor feedback, and γ_{CO_2} is the radiative forcing associated with a doubling of CO_2. The OLR in these formulae is computed using an offline radiation model, with temperature and humidity profiles derived from the simulations. Leaving aside changes in absorbed solar radiation or dynamical heat transports, maintainence of energy balance requires $\Delta OLR = 0$, whence

$$\Delta T_a = -\frac{\gamma_{CO_2}}{\gamma_T + \gamma_w} \Delta \log_2 (pCO_2) \tag{6}$$

From this equation, we see that the warming is proportional to the CO_2 radiative forcing, but with a sensitivity coefficient that is sensitive to both the water vapor changes and the temperature profile. Since γ_T is always positive and γ_{CO_2} is negative if temperature decreases with height, a negative γ_w enhances the warming.

[26] Table 1 shows the sensitivity coefficients based on the zonal mean temperature and humidity profiles taken from the simulations at 33S in January, near the latitude of maximum temperature. The first thing one notices is that, except at very high CO_2, the CO_2 radiative forcing is weak compared to the values familiar from the modern situation (about 4 W/m^2 per doubling). This is because of the weak vertical temperature contrast, and correspondingly the increase in radiative forcing is primarily due to an increase in tropopause height as the climate warms. γ_w is only about a tenth of γ_T, whence water vapor feedback produces only a slight enhancement of climate sensitivity. In contrast, water vapor feedback in the modern climate increases climate sensitivity by at least a factor of two. The climate sensitivity in the denominator of equation (6) is dominated by γ_T, which takes on values somewhat smaller than those of the modern world. This modest enhancement of dry climate sensitivity is a direct consequence of the cold temperatures of the hard snowball. For a blackbody surface of temperature T sitting in a vacuum, $\gamma_T = 4\sigma T^3$, whence we can define an effective radiating temperature for the level governing OLR changes by setting the no-atmosphere expression equal to the actual value of γ_T. The results are shown in Table 1, and correspond to cold, midtropospheric values. The simple lesson to be learned from this table is that our hard snowball climates remain cold because the CO_2 radiative forcing is weak, and the climate sensitivity also weak because of the feeble water vapor feedback.

[27] The cloud greenhouse effect (Figure 6) is also weak, for two robust reasons: (1) The cloud greenhouse effect arises from high clouds, but there is little water with which to make clouds in the cold upper summer atmosphere, or at any level in the winter hemisphere. (2) The weak summer meridional temperature gradient cannot support the baroclinic eddies that lead to midlatitude storm-track clouds in the modern climate. Significant cloud cover is limited primarily to the upward branch of the Hadley circulation, around 20° in the summer hemisphere. The zonal mean cloud greenhouse effect barely reaches 10 W/m^2, as compared to approximately 70 W/m^2 in the modern climate. Further, although the opposing cooling due to the cloud visible albedo is not as pronounced in the snowball case as it is in the modern climate, it is by no means negligible,

t1.1 **Table 1.** Clear-Sky OLR Sensitivity Coefficients for the Indicated CO_2 Ranges, Based on January Zonal Mean Conditions at 33°S Latitude[a]

t1.2 CO_2 Range	γ_T	γ_w	γ_{CO_2}	T_{rad}
t1.3 100–400 ppm	2.453	−0.320	−0.895	221.1
t1.4 400–1600 ppm	2.318	−0.319	−0.977	217.0
t1.5 1600–12,800 ppm	2.67	−0.294	−1.547	227.6
t1.6 12,800 ppm to 0.1 bar	3.093	−0.364	−3.677	238.9
t1.7 0.1–0.2 bar	2.952	−0.409	−6.194	235.2

t1.8 [a]T_{rad} is the effective radiating temperature of the level governing OLR changes. See text for definitions of the terms.

particularly over the relatively dark bare tropical ice. For example the maximum net cloud forcing for the .2 bar case is only 6.5 W/m^2, and the global mean net cloud forcing is a mere 2.5 W/m^2 (as compared to the temperature and latitude independant net cloud forcing of 15.56 W/m^2 assumed in CK92). We note that the simulated cloud forcing does increase with temperature, and therefore represents a positive feedback amplifying the warming. This effect may become progressively more important as temperature is further increased, either through addition of more CO_2 or through other radiative influences.

[28] Cloud effects present a notoriously formidable challenge to almost all climate simulation efforts. The situation for the hard snowball climate is not quite as dire as it is for climates more like the present. Much of the difficulty with getting cloud effects right for the present climate stems from the fact that the cloud albedo and cloud greenhouse effects nearly cancel, yielding a small result which is the sum of two large terms; a moderate error in either term can yield a large proportional error in the net cloud forcing. In the hard snowball case, the cloud forcing is dominated by the cloud greenhouse effect, because of the high albedo of the underlying surface. Hence the net cloud forcing is no longer a small residual of two large terms. All other things being equal, this reduces the error in the net cloud forcing relative to the typical magnitude of the net. For example, in the modern climate, even the sign of cloud feedback is in doubt, whereas in the hard snowball case it is virtually certain that clouds warm the climate.

[29] One should not thereby conclude that it is unimportant to get the clouds right. The CCM3 cloud parameterization used in FOAM is highly empirical, and while it performs satisfactorily over the range of temperatures encountered in the modern climate, it is not based on fundamental microphysical considerations. Thicker clouds cannot be ruled out solely on the basis of moisture availability. It takes very little moisture to make a optically thick cloud, and even in cold snowball conditions there is sufficient water vapor at low levels in the summer hemisphere to substantially increase the cloud longwave forcing, if only it could be transported to high levels and kept in suspension as condensed water. For example, in the .2 bar case, the subtropical precipitable water is on the order of 700 g/m^2, whereas it takes only 20 g/m^2 to make a cloud with an infrared emissivity of 80% [*Mahesh et al.*, 2001b]. In the hard snowball climate, convection is weak and injection of water aloft would be more sluggish than at present, so it would be expected that less of the available water (which is, in turn, much reduced in comparison to the modern climate) will be made into cloud water. However, the amount of cloud water that stays aloft depends ultimately on the rate of conversion to precipitation, and it is not completely out of the question that this factor could be lower in the snowball world. A better understanding of the behavior of the condensed water path in a hard snowball climate is clearly needed, and could perhaps be approached via detailed microphysical or cloud-resolving simulations of convection under cold conditions. A further discussion of the cloud parameterization, and some experiments exploring the sensitivity of the results to assumptions about cloud water content are presented in section 7.

4. Synoptic Eddy Heat Transport

[30] As noted in the Introduction, dynamic heat transports influence deglaciation through their effect on the latitudinal temperature distribution. In the midlatitudes, the transport is predominantly carried out by transient baroclinic (or "synoptic") eddies. These eddies draw their energy from the potential energy associated with the meridional temperature gradient, and they will therefore be greatly affected by the strong seasonal cycle of the temperature pattern. An introduction to the subject may be found in *Pierrehumbert and Swanson* [1995]. For the cold snowball climate, energy transport by latent heat is negligable, and only the dry static energy flux needs to be considered. This is given by $F_{trans} = g^{-1}\langle c_p T' + gZ'\rangle$, where c_p is the specific heat of air, T is temperature, Z is the height of a pressure surface, g is the acceleration of gravity, and angle brackets denote an integral with respect to distance over the latitude circle and with respect to pressure in the vertical [*Pierrehumbert*, 2002; *Trenberth and Caron*, 2001]. We shall define transients with respect to the monthly mean, so primed quantites refer to deviations from the corresponding monthly mean quantity. F_{trans} gives the rate of energy transport across a latitude circle, measured in units of power (typically petawatts, i.e., 10^{15} watts).

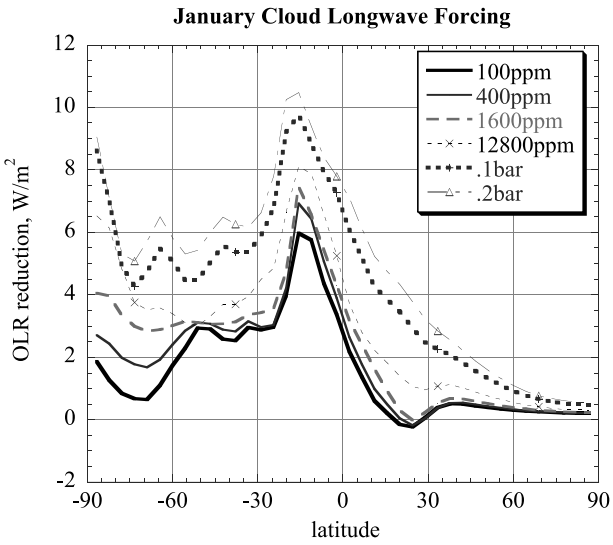

Figure 6. January zonal mean cloud longwave forcing, for various CO_2. The cloud longwave forcing is defined as the reduction in OLR caused by cloud effects, beyond the reduction caused by the clear-sky greenhouse effect.

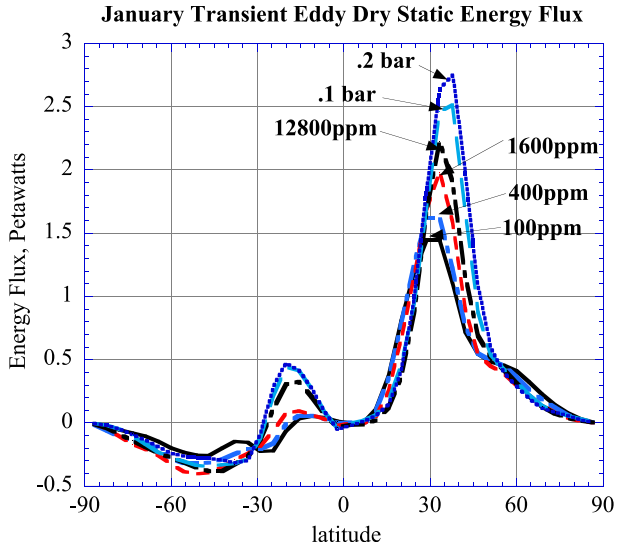

Figure 7. January transient eddy dry static energy flux, for various CO_2. Transient eddies are defined as the deviation from the monthly mean.

[31] Results for January are shown in Figure 7. Consonant with the analogy with Mars [*Walker*, 2001], synoptic eddy transports are primarily a winter phenomenon. While they play some role in smoothing out the warm bump near 30S in the summer hemisphere, the fluxes there are very weak compared to those in the winter hemisphere. The winter fluxes are sharply peaked near 30N, and decay rapidly poleward of this latitude. An examination of the full seasonal cycle (not shown) indicates that as the year progresses the flux makes a smooth and continuous transition between its winter and summer pattern. This is unlike the Martian storm tracks, which switch on precipitously during the autumnal equinox [*Collins et al.*, 1996].

[32] From the standpoint of deglaciation, the synoptic eddies are important because they draw energy out of the winter subtropics and cool it; the Hadley cell communicates this cooling throughout the tropics. Interestingly, the transport into the winter hemisphere increases from about 1.5 to 2.5 petawatts as CO_2 is increased from 100 ppm to .2 bars, despite the fact that the temperature gradient poleward of 30N changes little. The increasing temperature of the summer subtropics does increase the gradient between 15N and 30N, which may be governing the transport. However,there may also be important static stability effects, as detailed below. It is also interesting to note that the peak winter transient eddy fluxes are comparable to the approximately 2 petawatts of dry static energy fluxes in the modern climate [*Pierrehumbert*, 2002]. The modern atmosphere manages to transport a total of about twice this amount, by adding another 2 petawatts of latent heat transport. Thus the winter hemisphere eddy transport situation is rather like that of the modern climate, except that the latent heat flux has disappeared because of the low water content of the cold snowball atmosphere. It should be noted, however, that 2 petawatts of transport is more consequential in the snowball case than it would be in the modern climate, since the weak solar absorption of the reflective ice surface means that less energy transport is needed to compensate for the gradient in radiative heating between pole and tropics.

[33] The strong static stability of the winter hemisphere plays an important role in suppressing baroclinic eddies away from the subtropics. This can be seen from an examination of the "Charney Parameter," β^*, derived from linear instability theory [*Held*, 1978; *Pierrehumbert and Swanson*, 1995]. The parameter is given by $\beta^* = \beta L_d^2/(U_z H)$, where β is the gradient of the Coriolis parameter, H is the scale height, and U_z s the typical vertical wind shear. The radius of deformation is $L_d = NH/f$, with N being the Brunt-Vaisala frequency and f the Coriolis parameter. When $\beta^* \ll 1$ the beta effect is relatively unimportant, the eddies are as deep as the whole troposphere, and the characteristic horizontal scale is the radius of deformation. The modern extratropics, with $\beta^* \sim .2$ is in this regime. However, the winter extratropics in the hard snowball is vertically isothermal at around 200 K, yielding $N = g/\sqrt{RT} = .04\ s^{-1}$, $L_d = 2400$ km, and $\beta^* \sim 3$. In this regime, the beta effect suppresses longwave, deep eddies and the modes are comparatively shallow and weak. In lieu of the radius of deformation, the characteristic horizontal scale is the Rossby scale $(f/N)(U_z/\beta)$, which works out to about 800 km for the snowball extratropics. Coincidentally, this is about the same as the radius of deformation for the modern extratropics, implying similar horizontal scales for the eddies in the two cases. However, in the snowball case, the characteristic depth scale is a shallow 2 km, and the typical growth rate is $(f/N)U_z$, smaller than that of the modern climate by virtue of the large value of N. The expectation that the simulated eddies are shallow and of a scale less than L_d needs to be probed with further diagnostic analyses; that is an intricate subject, which will be left to future work. The relevance of linear stability theory to the nonlinear baroclinic turbulence of the atmosphere is at best uncertain, but stability theory is sufficient to show that, despite a temperature gradient comparable to the modern winter, the hard snowball winter climate is in a very different baroclinic regime than the present one.

[34] To what extent can the behavior of the dynamic heat transport be captured by a diffusive EBM? The direction of heat transport is consistently downgradient, and in that sense consistent with diffusion. However, the magnitude of the transport is clearly not proportional to the local temperature gradient. It is nonetheless instructive to compute the range of effective thermal diffusivities implied by the simulation, and to assess the errors in estimating the maximum flux by a diffusive approximation. To do this, we find, for each CO_2 case and for each month, the maximum F_{trans} in each hemisphere, and then compute the mean temperature gradient averaged within 10 degrees latitude on either side of the location of the maximum flux. Using these values, the diffusivity D is then defined according to the relation

$$2\pi r_e^2 D \cos\phi \frac{\partial T}{\partial \phi} = F_{trans} \qquad (7)$$

where r_e is the Earth's radius and ϕ is the latitude. If F_{trans} is measured in Watts, then D will have units of W/(m^2 K), and will be consistently with usage in EBMs such as described in CK92. In Figure 8 we show a scatterplot of each estimate

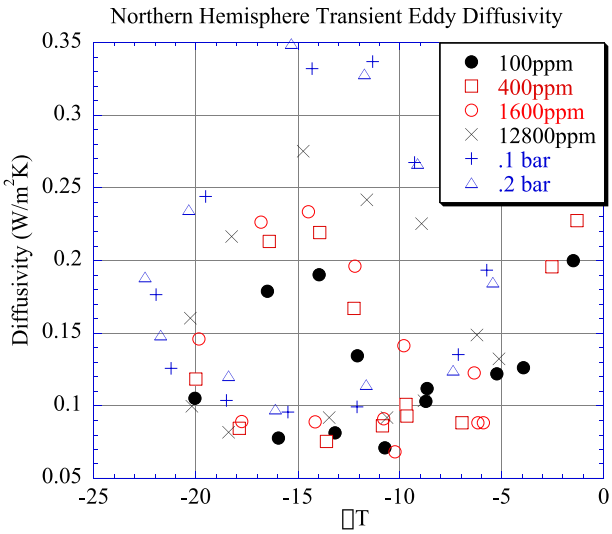

Figure 8. Scatterplot of Northern Hemisphere thermal diffusivity diagnosed from the simulations, against temperature difference over the interval extending 10 degrees of latitude on either side of the point of maximum dry static energy flux. Each point represents an estimate for an individual month, for the indicated value of CO_2.

of D versus the temperature difference between 10 degrees of latitude N and S of the point where the estimate is made. Only Northern Hemisphere results are shown, since results for the Southern Hemisphere are essentially the same except for reversal of the sign of ΔT. The diffusivity is far from constant; it varies by a factor of three or more. A detailed examination of the seasonal cycle (not shown) reveals that the largest values occur near the spring equinox in each hemisphere, while the smallest values occur near the autumn equinox. This is indicative of a static stability effect, as the atmosphere is more convective, and has lower static stability, when it is warming (spring) than when it is cooling (autumn). The winter values of diffusivity are intermediate between the extremes, and are on the order of .2 W/(m^2 K). This is less than a third of the value used in CK92 and many other energy balance models, based on making the model reproduce the modern climate. It should be no surprise that the hard snowball diffusivity is much lower than that appropriate for the modern climate, owing to the lack of latent heat transport. The drop in diffusivity is actually somewhat greater than one would expect on moisture considerations alone. Whatever the cause, the relatively low diffusivity is a favorable factor for deglaciation, since it means that less tropical heat gets bled off into the extremely cold winter hemisphere than would be expected from EBM estimates. It would not, however, be appropriate to use the same low diffusivity in the tropics, as the heat transport there is governed by quite different mechanisms.

[35] Nonlinear scaling theory for baroclinic turbulence is a very unsettled subject, but such theories as there are invariably imply that the eddy diffusivity should vary with both the static stability and temperature gradient. A summary of the principal extant results can be found in *Barry et al.* [2002]. None of the parameterizations cited in *Barry et al.* [2002] has proved unambiguously successful when applied to the real atmosphere or realistic simulations, but the results of *Held and Larichev* [1996] are of particular interest because they derive from a precise turbulent scaling theory, albeit applied to a statistically homogeneous baroclinic zone rather unlike the limited baroclinic zones of the real atmosphere. In this theory, the diffusivity is proportional to $L_d/(\beta^*)^2$, and hence should vary like L_d^{-3} for fixed vertical shear. In agreement with arguments based on linear stability theory, the scaling theory predicts a strong suppression of baroclinic eddies as static stability is increased; in fact, a doubling of N should reduce the eddy diffusivity by a factor of 8. This result again underscores the importance of static stability in determining the heat flux, but our attempts to make a more precise comparison between the simulations and the scaling predictions proved ambiguous, because of horizontal inhomogeneities in both the temperature gradient and static stability. *Barry et al.* [2002] proposed a new scaling theory, which appears to succeed remarkably at reproducing GCM simulations over a wide range of conditions. However, the new theory is not in itself usable as a parameterization scheme, as it is partly diagnostic; it actually requires the net energy transport across the baroclinic zone as an input to the scaling law. Static stability does not appear explicitly in the expression for diffusivity, but enters only implicity through the net energy transport (see Table 1 of *Barry et al.* [2002]), which must generally be computed from simulations or some other parameterization.

[36] Given the present state of scaling theory, there is little hope for reliable treatment of heat transport in simplified models of the snowball climate. The challenge of formulating a parameterization that can reproduce the transport behavior in the hard snowball climate can serve as both stimulus and testbed for further developments of scaling theory.

5. Hadley Cell

[37] In the tropics, the dynamic heat transport is predominantly carried out by the Hadley circulation, a zonally symmetric overturning cell which changes gradually over the course of the seasonal cycle. In fact, dynamically speaking, "the tropics" may be defined as that region of the globe where the Hadley cell plays the dominant role in determining the temperature pattern. Weak Solar forcing, low thermal inertia of the surface and the very limited role of latent heat transport in a cold, dry atmosphere, could cause the Hadley cell on a hard snowball Earth to differ markedly from that of the present climate. In the modern world, the Hadley cell homogenizes free-troposphere temperature between about 20N and 20S, causing this region to behave as a single thermal unit; substantial gradients in atmospheric heating are redistributed so as to yield weak variations in tropical temperature. In particular, the vertical profile of temperature lies on the moist adiabat both in the convective region and the subsiding region, despite the fact that active convection occupies only a small portion of the tropics [*Pierrehumbert*, 1995]. Our goal in this section is to describe the extent to which the effects of the hard snowball Hadley circulation deviate from this picture.

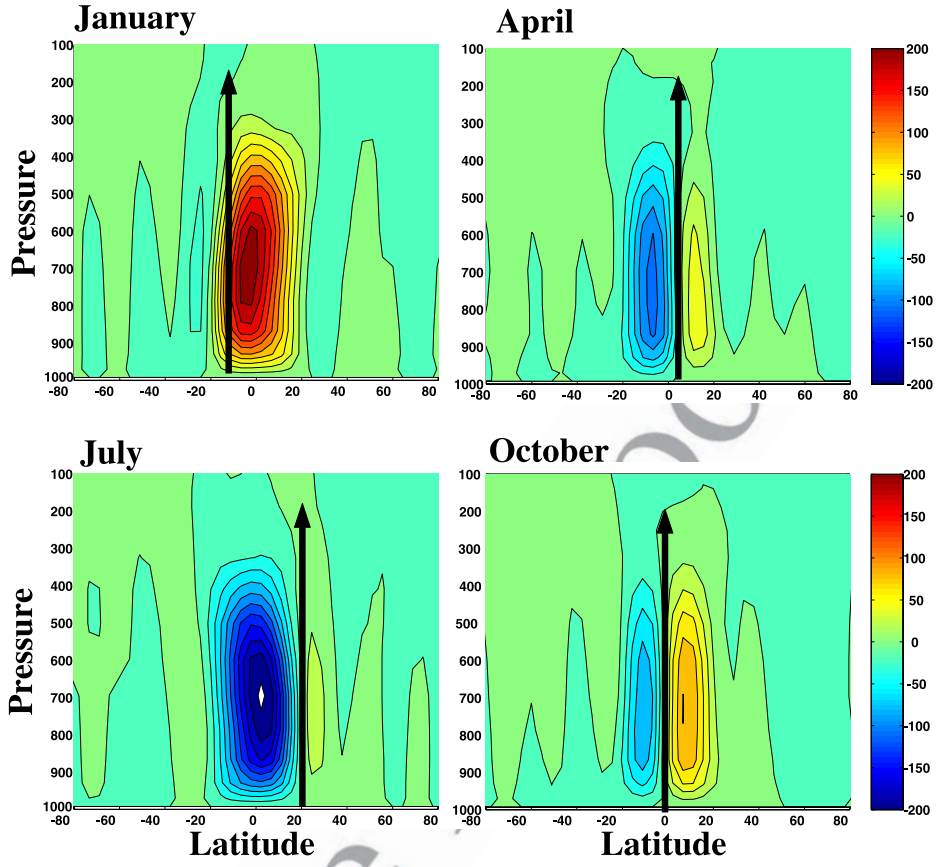

Figure 9. Seasonal cycle of the mass flux streamfunction of the Hadley circulation, for the case with 100 ppm CO_2. Units are 10^9 Kg/s. The contour interval and color scale are the same for all panels.

[38] We begin with a basic description of the zonal-mean circulation, the mass-flux streamfunction of which is shown in Figure 9 for the 100 ppm climate. The streamfunction is defined such that the streamfunction difference between any two contours is the rate of mass flow carried by the Hadley cell in the region between those contours. If one attributes roughly half the mass of the atmosphere to the tropics, then a Hadley cell with maximum streamfunction value of 200 $\times$ 10^9 Kg/s would turn over the tropical atmosphere in approximately 150 days.

[39] The general pattern is similar to that of the present-day cell. The cell is strongest near the times of the solstices, and at those times takes the form of a single cell with a rising branch in the summer subtropics and a subsiding branch in the winter subtropics. Thus the circulation reverses direction between the two solstices. As the equinox is approached, the circulation takes on a two-cell pattern with rising motion near the equator, but it is very weak. As pointed out by *Lindzen and Hou* [1988], the two-cell pattern one obtains by taking an annual average is rather misleading, and the Hadley cell is best thought of as a single-cell pattern carrying heat from the summer to the winter subtropics. The compressional heating in the subsiding branch causes the atmosphere there to be warmer than it would have been in local radiative-convective equilibrium, and is the primary means by which the Hadley cell acts to homogenize the tropical temperature. There is a compensating local cooling in the ascending region. The cooling (relative to the local radiative equilibrium temperature) in the ascending branch is due to import of air with low potential temperature by the low level flow, and not to adiabatic expansion of the rising air. Convection keeps the ascending region on the adiabat (dry or moist), and ascent along an adiabat does not change the temperature profile. This is equally true for the present moist Hadley circulation as it is for the dry snowball one. The biggest difference in the physics of the snowball circulation comes in the subsiding region. For the modern case, the moist and dry adiabats differ greatly, and air ascends along the moist adiabat but descends under the influence of dry adiabatic compression and infrared cooling alone. Therefore it is possible to have compressional heating in the subsiding branch even if the temperature profile is on the moist adiabat in both cases. For the dry snowball circulation, there is essentially no asymmetry between ascent and descent, so compressional heating could not occur in the subsiding region if it relaxed to the same dry adiabatic profile obtaining in the ascending region.

[40] A quantitative comparison to the modern day Hadley cell is instructive. We computed the monthly composited mass flux streamfunction from NCEP data [*Kalnay et al.*, 1996] for the years 1967–1987. Surprisingly, the 100 ppm hard snowball Hadley circulation is actually stronger than the modern one, and carries a flux of 215 $\times$ 10^9 Kg/s in

t2.1 **Table 2.** January Hadley Cell Characteristics[a]

t2.2 CO_2	ψ_{max}, 10^9 Kg/s	ϕ_S	ϕ_N
t2.3 100 ppm	215.	−15.6	15.6
t2.4 400 ppm	211.	−15.6	15.6
t2.5 1600 ppm	222.	−15.6	15.6
t2.6 12,800 ppm	240.	−20.0	15.6
t2.7 0.1 bar	311.	−20.0	15.6
t2.8 0.2 bar	344.	−20.0	15.6

t2.9 [a]ψ_{max} is the maximum streamfunction value, and measures the net mass flux of the circulation. ϕ_S and ϕ_N are the latitudes of the southern and northern boundaries of the Hadley cell, defined as the most poleward latitudes at which the streamfunction attains 20% of its maximum value.

January versus only 167×10^9 Kg/s for the modern January case. The 100 ppm hard snowball circulation is shallower than the modern case; its center, as measured by location of the maximum streamfunction is near 700 mb, versus 500 mb for the modern case, and its top as measured by the layer containing 80% of the mass flux is 325 mb, versus 100 mb for the modern case. The poleward limit of the rising branch in the summer hemisphere is not too different between the two cases (15.5S latitude in January for the 100 ppm case, versus 12.5S for the modern case). However, the penetration of the descending branch into the winter hemisphere is much more limited for the hard snowball case than the modern case (15.5 N for 100 ppm in January, versus 27.5N for the modern case).

[41] As shown in Table 2, the Hadley circulation is only weakly sensitive to massive changes in the CO_2 content of the atmosphere. As the climate warms, the strength of the circulation increases moderately and the rising branch penetrates very slightly further into the summer hemisphere. The sinking branch remains fixed. Further, the depth of the circulation (not shown in the table) changes little from the values quoted previously for the 100 ppm case.

[42] The Hadley cell is vigorous, but not sufficiently vigorous to homogenize the tropical temperature to the extent prevailing in the modern climate. This is evident in the surface temperature pattern shown in Figure 3. The temperature aloft (not shown) also varies considerably across the tropics. In particular, the Hadley cell fails to relax the entire tropics to the adiabat; the vertical profile is on the dry adiabat in the ascending branch, but has substantial static stability in the subsiding branch. A full inquiry into the physics limiting the strength of the circulation confronts intricate dynamical issues, and would lead us far afield from the immediate task at hand. More comprehensive diagnostics, and a detailed dynamical analysis, will be provided in a separate paper (R. T. Pierrehumbert, manuscript in preparation, 2005). The principle factors at work are as follows: (1) The snowball Hadley state (as well as the modern one) does not attain the equilibrium constant angular momentum state having temperature symmetry across the equator. Both transient and eddy effects are involved. The circulation is only guaranteed to eliminate the temperature gradient in a narrow zone near the equator. Elsewhere, the gradient depends on the strength of the differential heating. (2) Owing to the absence of the thermal inertial of an open tropical ocean, the cross-tropical gradient in atmospheric heating is considerably greater in the snowball case than it is in the modern climate. The snowball Hadley circulation cannot become strong enough to even out the effects of such strong differential heating. (3) The virtual absence of moist effects eliminates the asymmetry between upward and downward motion, and renders the state with a dry adiabat across the entire tropics energetically inconsistent.

[43] Though the Hadley cell is unable to eliminate tropical temperature gradients in the snowball climate, it is nonetheless strong enough to have a profound effect on the tropical temperature pattern. In January in the .2 bar case, for example, the Hadley cell draws about 30 W/m^2 of energy out of the ascending region, near 20S. This is deposited in the subsiding region, where it is largely carried away to the cold winter hemisphere by synoptic eddies. For the deglaciation problem, it is particularly significant that the Hadley cell carries heat away from the equator at a rate of 20 W/m^2 or more throughout the year. This heat loss helps to keep the annual mean equatorial temperature cold, and inhibits deglaciation.

[44] Since subsurface ice temperature and hence deglaciation are primarily sensitive to the annual mean temperature, it is natural to wonder whether a steady theory of Hadley circulations forced by the annual average insolation would suffice. If the Hadley cell dynamics were linear, this would unquestionably be the case. However, the angular momentum transport which figures prominently in the theory of *Held and Hou* [1980] makes the problem nonlinear. The extent to which this nonlinearity affects the annual mean climate in an oscillating Hadley circulation is at present unclear, and must await a mathematical analysis of the time-dependent case.

6. Hydrological Cycle and the Surface Energy Budget

[45] The precipitation-evaporation budget is of interest because it governs the distribution of snow cover, because it is affects sea-glacier flow, and because it defines the net

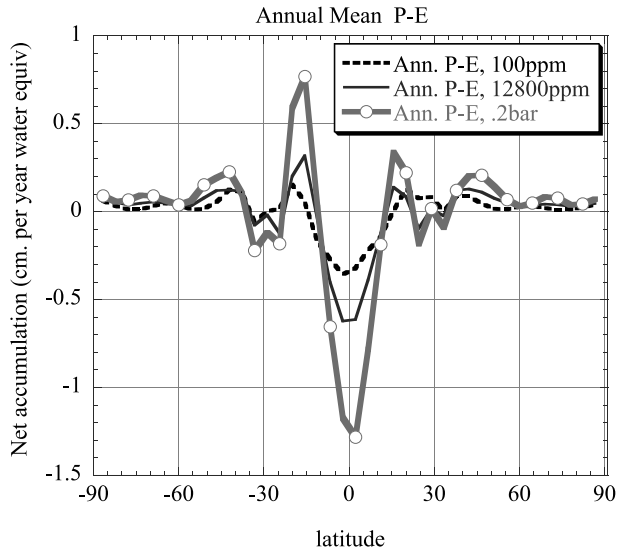

Figure 10. Annual-zonal mean residual of precipitation over evaporation for various CO_2 concentrations. Units are cm/year of liquid water equivalent.

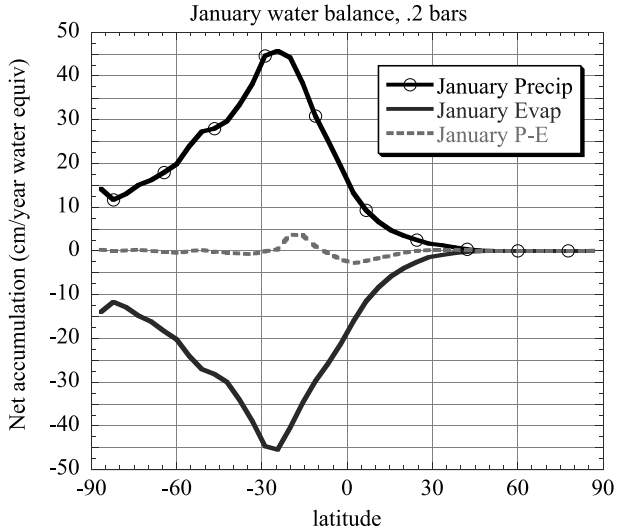

Figure 11. January precipitation, evaporation and residual for the .2 bar case.

ablation zones where sea ice may be relatively thin. Annually and zonally averaged $P - E$ statistics are shown in Figure 10. As expected from previous simulations, and from basic thermodynamic arguments [*Pierrehumbert*, 2002], the accumulation rate is very small, under a centimeter per year of liquid water equivalent, increasing modestly as CO_2 and temperature increase. The region from about 10N to 10S is a net ablation zone, where new water vapor enters the atmosphere by evaporation from sea ice, which in turn is replenished by freezing at the base. Most of this is snowed out in strong accumulation zones near 16N and 16S, due to moisture convergence in the upward branch of the Hadley circulation at the solstices. There is also some weak accumulation poleward of 35N and 35S. These two accumulation zones are separated by a region of of very weak net ablation or accumulation. The positions of the accumulation and ablation zones change little as CO_2 is changed. Although the net accumulation seems unimpressive, over the lifetime of the hard snowball it is highly consequential; acting relentlessly for a million years, a 1 cm/yr accumulation would yield a 10 km high ice dome, if uncompensated by flow of sea or land glaciers.

[46] The small net accumulation is actually the residual of a much larger precipitation and evaporation, as indicated by the January data in Figure 11. At .2 bars, the precipitation and evaporation individually occur at a rate of about 40 cm of liquid water equivalent per year. There is very little synoptic variability in the summer hemisphere, and most of the local recycling of water occurs in the course of the diurnal cycle. There is a pool of about 1 mm of water in the form of snow or ice, which evaporates into the atmosphere each afternoon and snows out almost immediately, before it has a chance to be transported. Even this modest evaporation is far in excess of what would be possible were the surface temperature constant at around 250 K throughout the day. It is only possible because of the large diurnal cycle, which arises because of the low thermal inertia of the surface (compounded by the extremely low diffusivity of snow cover). The ice and snow surface warm greatly in the afternoon, leading to low boundary layer relative humidity, which helps sustain relatively large evaporation rates. The diurnal cycle also has a marked effect on the surface energy budget as will be discussed shortly.

[47] During the short simulations reported here, snow only builds up to a modest depth on the order of a meter of liquid water equivalent. The equilibrium snow depth could only be determined if ice and sea glacier dynamics were taken into account, but the present simulations are more than adequate for determining the snow albedo feedback. Observations show that it only takes 5–10 mm, of physical snow depth to reset the ice surface albedo to that of snow [*Warren et al.*, 2002]. FOAM treats the snow albedo affect somewhat more conservatively than this, assuming that the surface albedo approaches that of snow gradually, at a characteristic depth dependant on the surface roughness. Over ice, surface albedo reaches half of its maximum value at a physical snow depth of 4 cm (or. 4 cm of liquid water equivalent), and is nearly saturated at a physical depth of 8 cm. Apart from the role of sea glacier flow in replacing bare sea ice with glacier ice, the surface albedo can be regarded as being in equilibrium. The snow depth pattern is shown in Figure 12. There is a narrow band of bare ice near the equator, and two major bands of deep

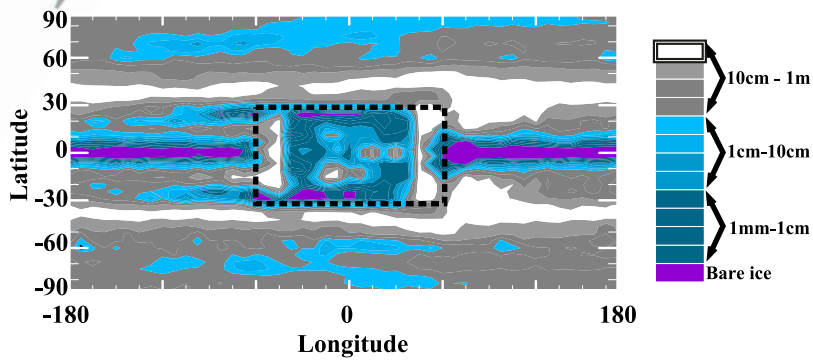

Figure 12. Distribution of annual mean snow depth (liquid water equivalent) in the final year of the .2 bar run. Snow accumulation in the model is capped at 1 m liquid water equivalent. Regions which have reached this limit by the end of the simulation are shown in white. Regions of bare ice or ground are colored with violet. The bold dashed line delineates the equatorial supercontinent.

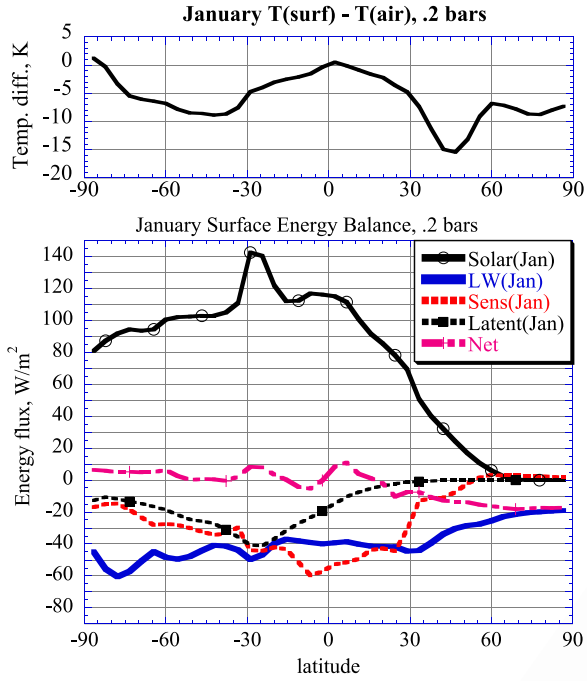

Figure 13. (top) January temperature difference between the surface and the overlying air for the .2 bar case (negative values correspond to suface colder than air). (bottom) Corresponding surface energy budget. Curves give the absorbed solar radiation (Solar), net infrared cooling (LW), cooling due to sensible heat flux (Sens), cooling due to latent heat flux (Latent), and the residual net flux (Net).

snow at the edge of the tropics. The polar regions have very light snow cover, but it is sufficient to cause a substantial increase in the albedo there. Apart from snow accumulation in the coastal mountain ranges, the tropical continent remains largely devoid of snow. Because of the greater surface roughness over land, the modest snow cover there is has only a minor effect on the continental albedo.

[48] The snow accumulation at the edge of the tropics affects sea glacier flow, but it should not be concluded that the primary glacial flow is away from these two regions. Sea glaciers are largely driven by pressure gradients due to the formation of thick ice in the cold polar regions, where the ocean loses energy relatively quickly owing to the large temperature difference between the ice surface and the unfrozen water below. For a typical high latitude mean temperature of 200 K, the balance between diffusive heat loss through the ice and latent heat release by basal freezing yields a growth of nearly 15 cm per year for an initial ice thickness of 100 m, and 1.5 cm per year for 1 km thick ice. Even the latter dominates thickness growth by snow accumulation, so sea glacier dynamics would most likely carry the snow mounds into the deep tropics, increasing the albedo there.

[49] The surface energy budget sheds some further light on the diurnal cycle alluded to earlier. This cycle is worth closer study, because it turns out to have an important cooling effect on the mean ice surface temperature. In the top panel of Figure 13, we show the difference between the surface temperature and the temperature of the overlying air, in January (negative values corresponding to ice colder than air). The mean surface temperature is up to 10 K colder than that of the overlying air, with particularly large differences occurring over the midlatitude deep snow belts. We show the corresponding surface energy budget in the lower panel of the figure. As expected from the low thermal inertia of the surface, the residual of the surface budget is nearly zero, except at the winter pole where the surface hasn't come completely into equilibrium, owing to the slow radiative cooling at such low temperatures. The real surprise is that the sensible heat flux is out of the surface and into the atmosphere, and thus appears to be countergradient. Given the bulk heat transfer formula used in FOAM, this would be impossible if the surface temperature were constant at the monthly mean. This seemingly bizarre state of affairs is in fact a simple result of the rectification of the large diurnal fluctuation of surface conditions by the nonlinearity of the Monin-Obukhov parameterization of turbulent transfer of sensible and latent heat. During the daytime, the surface temperature becomes up to 10 K warmer than the air temperature, and there is substantial upward transfer of heat through the unstable boundary layer. At night, however, the boundary layer becomes stably stratified, cutting off virtually all turbulent heat transfer. The surface is warmed only by the downwelling infrared radiation from the atmosphere, which is weak owing to the dry optically thin atmosphere, and hence plummets to extremely cold temperatures quickly because of the low thermal inertia of the surface. The effect is especially marked over regions of deep snow cover, because the thermal diffusivity of snow is far less than that of ice, whence the surface attains its very cold equilibrium temperature more quickly. Over snow, the night time temperatures can be 20 K lower than the air temperature. This is an unanticipated effect of snow cover, above and beyond the albedo effect, which further inhibits deglaciation.

[50] The strong diurnal cycle seen in these simulations supports the interpretation of tropical Neoproterozoic sand wedges proposed by *Maloof et al.* [2002]. The formation of sand wedges requires strong temperature variations over a suitable timescale; if the timescale is too short, the temperature wave is too shallow to form sand wedges, whereas if the timescale is too long, viscous relaxation of the soil prevents the buildup of stresses that lead to cracking and subsequent formation of the wedges. Currently, sand wedges form as a result of synoptic systems in high latitude regions characterized by large temperature gradients and high seasonality, and, as reviewed in *Maloof et al.* [2002], the existence of Neoproterozoic tropical sand wedges is sometimes taken as support for very high obliquity, which would lead to high tropical seasonality. Given that sand wedges form as a result of synoptic activity, rather than the slow seasonal temperature variation, the high obliquity interpretation is partly founded on a dynamical misconception, as midlatitude-style synoptic eddies are not to be expected in the tropics even in the high obliquity case, owing to the low coriolis parameter there. *Maloof et al.* [2002] show, on the other hand, that in snowball Earth conditions sand wedges could form as a result of the diurnal cycle, if the diurnal temperature range on the order of 20 K or more. Given the strength of the diurnal cycle seen in our

t3.1 **Table 3.** Sensitivity of the Maximum January and Annual-Averaged Ice Surface Temperatures to Selected Modeling Assumptions, Accompanied by Corresponding Solar Absorption Statistics[a]

t3.2 Case	Max Jan. T_{ice}	Max Ann. Avg. T_{ice}	α_{toa}	$\alpha_{toa,clr}$	Jan. Summer S_{abs}
t3.3 0.2 bar control	247.8	243.9	0.664	0.654	157.6
t3.4 Spectral albedo	247.7	243.9	0.664	0.654	157.2
t3.5 Dark ice	247.9	243.8	0.664	0.654	157.5
t3.6 Thin snow	262.5	246.0	0.613	0.598	194.4
t3.7 Dark snow	264.0	247.9	0.618	0.601	183.4

[a] α_{toa} is the all-sky January albedo averaged over the illuminated portion of the globe, $\alpha_{toa,clr}$ is the corresponding clear-sky albedo, and S_{abs} is the January mean solar absorption averaged over the summer hemisphere. The "spectral albedo" case was carried out with a shortwave ice albedo of 0.6 and a longwave ice albedo of 0.4. In the "dark ice" case each of these albedos was reduced by 0.1. "Thin snow" was carried out with the same ice albedo as "dark ice" but with artifically reduced snow cover. "Dark snow" used the same ice albedo as "spectral albedo," but reduced the longwave and shortwave snow albedo by t3.8 0.1 each relative to the control case. All experiments were carried out with 0.2 bars of CO_2.

simulations, the interpretation of *Maloof et al.* [2002] emerges as the most plausible explanation of the sand wedges. Indeed the requirement of a strong diurnal cycle supports the notion of a hard snowball, since open tropical ocean would tend to moderate the diurnal cycle over land, even if the land became cold enough to undergo freeze-thaw cycles. It should also be noted that, if the paleolatitude of the Neoproterozoic sand wedges is at the poleward range of its band of uncertainty, synoptic variability may also contribute to their formation. The strong winter hemisphere temperature gradients, and low thermal inertia of the frozen surface, allows significant synoptic variability to penetrate to within about 15 degrees of the equator, as evidenced by Figure 7.

[51] Another interesting consequence of the strong diurnal cycle is that it may help to provide freshwater refugia on tropical continents. Bare, dark land adjacent to glaciers can easily heat up during the day to temperatures above freezing, and could sustain some episodic melting of snow and glacier ice. This meltwater could feed tropical ice-covered lakes analogous to those presently found in the Antarctic dry valleys. Ice on such lakes could conceivably be kept thin enough to sustain photosynthetic life in the liquid layer below, along the lines discussed in *Warren et al.* [2002]. Refugia of this sort would not, of course, be pertinent to the survival of organisms which require a marine environment.

7. Sensitivity to Surface Albedo and Cloud Assumptions

[52] The sea-ice/snow surface is a complex material, and radiative transfer through this substance poses challenges as formidable as the better recognized challenges of clouds [*Warren et al.*, 2002]. To help identify the more important factors, we have carried out a number of simulations with alternate assumptions concerning surface albedo, holding CO_2 fixed at .2 bars. These simulations are summarized in Table 3. In this table, we give the annual mean maximum ice surface temperature, as well as the January maxima, since the former is most relevant to determining deglaciation.

[53] The bare ice albedo for the control case has a broadband value consistent with measurements reported by *Warren et al.* [2002], but the measurements show that ice is more reflective for short wave visible radiation than for near-IR. The importance of this effect is probed in the "spectral albedo" experiment, where we increase the ice albedo in the shortwave half of the solar energy spectrum to .6 and reduce it to .4 in the longwave half. This produces virtually no change in the climate, because the atmosphere only weakly alters the incoming solar spectrum, and because most of the ice surface is shielded by snow. The shielding by snow also accounts for the paucity of effect in our "dark ice" experiment, where we reduced the ice albedo to .5 in the shortwave and .3 in the longwave. Relatively bubble-free ice such as the marine ice rarely encountered at the surface in modern conditions could be this dark or darker [*Warren et al.*, 2002], but unless one finds a way to keep more ice free of snow, it will have little effect on the surface temperature.

[54] The next experiment reduces the snow albedo effect by arbitrarily changing the characteristic snow optical depth scale in the albedo parameterization from 4 cm to 10 meters, while keeping the ice albedo fixed at that of the "dark ice" experiment. This "thin snow" experiment is unrealistic, but serves to illustrate the importance of the snow cover, and also as a check of the amount of extra warming that would be obtained if the true precipitation field left much more bare ice than the simulations. The "thin snow" experiment shows a very substantial warming in the January maximum ice temperature; this temperature increases nearly 15 K in response to a 37 W/m^2 increase in absorbed solar radiation occasioned by the reduction in surface albedo. However, most of this warming occurs near latitude 30S, where it is offset by very cold wintertime temperatures. The warmest annual mean ice temperature occurs at the equator, and this warms only slightly. Part of the reason is that the deep tropical albedo reduces only slightly, because the albedo there is already dominated by bare land and bare ice. An additional reason is that the proximity of the equator to the very cold winter hemisphere holds down its temperature, through loss of heat to the cold regions.

[55] In the "dark snow" experiment we restore the original snow cover parameterization, but reduce the snow albedo to .8 in the shortwave and .5 in the near-IR (for a broadband reduction of .1). Such a reduction could perhaps be produced by admixture of dust with the snow. The low net snow accumulation favors albedo reduction by dust, since it would tend to increase the dust concentration in the snow, all other things being equal. However, when one recalls that the net accumulation is a residual of large evaporation and large precipitation, it does not seem so clear that dust could significantly reduce the snow albedo.

Any dust washed out of the atmosphere would be left behind as the snow evaporated in the daytime, only to be covered up almost immediately by a relatively heavy fall of fresh snow. Such issues can only be properly addressed through a quantitative dust transport and deposition model, but as a route to deglaciation "dark snow" suffers from the same problem as "thin snow." There is a substantial summertime warming, but only a moderate increase in the annual mean tropical temperature. In both the "dark snow" and "thin snow" cases, there is an interesting poleward redistribution of snowcover in response to the midlatitude summer heating, but the redistribution isn't extreme enough to substantially amplify the midlatitude warming.

[56] The preceding experiments may not exhaust the possibilities for reduced surface albedo, but they do indicate that rather extreme reductions would be necessary to trigger deglaciation at or near .2 bars. Set against this possibility is the high probability of a number of effects that could intervene to increase the surface albedo beyond that assumed in our control experiment. Sea glacier flow, as discussed in *Goodman and Pierrehumbert* [2003], would tend to replace the relative dark tropical bare sea ice with brighter glacier ice. Further, cold subeutectic ice is nearly as bright as snow, because of the formation of salt crystals which are effective scatterers [*Warren et al.*, 2002]. At .2 bars, the mean tropical ice temperature is near or below the eutectic, suggesting the formation of bright ice. However, the diurnal cycle can cross the eutectic, leading to a very unfamiliar situation that has yet to be studied theoretically. The formation of bright subeutectic ice represents a kind of barrier to deglaciation, since it will tend to keep itself cold enough to remain subeutectic. However, the importance of both the salt crystal effects and sea glacier effects is probably limited, because the surface albedo is so dominated by snow cover.

[57] A more serious threat to deglaciation is the prospect that the tropical continent, which is mostly bare in our simulations, might eventually become snow covered. Simulations with a land glacier model driven offline by GCM-simulated precipitation indicate that this is a distinct possibility [*Donnadieu et al.*, 2003]. While very dark ice or very dusty snow cannot be ruled out at this point, it generally appears that alternative models of surface albedo do not provide an easy route to deglaciation.

[58] Clouds constitute another parameterized process with considerable potential for affecting the outcome of the deglaciation experiments. A cloud parameterization must predict the vertical and horizontal distribution of fractional cloud cover, cloud particle size, and cloud condensed water content. It is the cloud water content that has the most leverage over deglaciation. The particle size primarily affects cloud albedo, the affect of which is attenuated by the already bright ice or snow surface. Reduced cloud cover could make deglaciation even harder, but the existing parameterization in FOAM already produces near-total cloud cover in convective regions, so there is little chance to favor deglaciation by this means. Increase in the cloud water content, however, could substantially increase the cloud greenhouse effect, which is by far the dominant cloud effect in the hard snowball climate.

[59] The version of CCM3 cloud water parameterization employed in FOAM is empirical rather than microphysical. It assumes that cloud water q_{clw} decays exponentially in height, with the law

$$q_{clw} = q_{clw0} e^{-z/H_{clw}} \tag{8}$$

where z is the altitude above the ground and the scale height H_{clw} is given in terms of the total column precipitable water q_{tot}, measured in millimeters, by the formula

$$H_{clw} = H_0 \ln(1. + q_{tot}) \tag{9}$$

In these formulae q_{clw0} and H_0 are empirical constants. The standard parameter settings are $H_0 = 700$ m and $q_{clw0} = .21$ g/m^3. This parameterization is based loosely on scattered observations suggesting an exponential decrease of cloud water with height, combined with tuning to fit the observed meridional distribution of cloud radiative forcing by making the scale height dependent on some simple characterization of atmospheric water content. For the hard snowball case, it is important to note that q_{clw0} is fixed independantly of the temperature or actual water content of the atmosphere, and therefore does not take into account the reduced supply of moisture in the cold climate of the snowball Earth. The reduction of cloud effects in the snowball comes about through the reduction in H_{clw}, occasioned by the radical drop in total precipitable water in the hard snowball atmosphere. A useful point of reference is that a cloud water concentration of 5 mg/m^3 spread over a 2 km thick cloud is sufficient to make a cloud with an infrared emissivity of 50% [*Mahesh et al.*, 2001b]. For the summer subtropics in the .2 bar case, the concentration falls to this value at an altitude of 1.4 km, and to 1 mg/m^3 at 2 km; by 4 km, the cloud water is completely negligible. The parameterization thus predicts low, thin clouds in the snowball summer tropics.

[60] We cannot very strongly defend the use of this cloud water parameterizaton for climates very different from the modern one. Some weak confidence may be taken from the fact that the parameterization does not produce radically wrong cloud effects in the cold polar regions of the modern climate, which have temperatures comparable to the snowball tropics. Still, the polar regions of the modern climate are not precisely analogous to the snowball tropics, as they lie in a rather different convective regime. Clearly, the whole problem of cloud water content in cold convective systems requires deeper inquiry, which is beyond the scope of the present work. In the meantime, to provide some general idea of the the sensitivity of deglaciation to cloud water content, we have performed an experiment with the base-case surface albedos and .2 bars of CO_2, but with the scale height parameter H_0 increased to 3500 m. This yields a cloud water scale height similar to that used in the model to reproduce modern tropical cloud forcing; it almost certainly yields an overestimate of the cloud forcing in the snowball atmosphere, especially given that q_{clw0} is also fixed at its modern value. We shall refer to this case as the "thick cloud" experiment.

[61] In the thick cloud experiment, the maximum January zonal mean cloud greenhouse effect occurs in the summer subtropics, as for the control case, but reaches 51 W/m^2; this value is only slightly less than the tropical zonal mean cloud

greenhouse effect in the modern climate. There is little increase in cloud forcing in the winter hemisphere, which is too cold to permit much cloud formation even with the increased scale height factor. Because much of the summer cloud cover occurs over the dark bare continent, the cloud albedo effect cancels a fair amount of the cloud greenhouse effect, reducing the maximum zonal mean net cloud forcing to 31 W/m^2. The global mean net cloud forcing is only 10 W/m^2. Still, the substantial local subtropical cloud forcing leads to a substantial increase in subtropical maximum temperature, which increases by fully 12 K at the ice surface, to 259.9 K. However, the warming of the annual mean maximum ice temperature (which occurs at the equator) is much weaker. The 5.1 K warming of this temperature increases the annual mean ice surface temperature only to 249.2 K, which is still far short of what is required for sustained melting. Thus it appears that extreme increases in cloud water content can bring the system close to the formation of transient summertime melt ponds, but do not bring the system to the threshold of deglaciation.

[62] How reasonable are the low, thin clouds predicted by the control-case parameterization, as compared to observations? One indication comes from ERBE satellite observations. Though it is difficult to discriminate clear sky from cloudy sky over ice, ERBE estimates over Antarctica suggest cloud longwave forcing ranging from under 2 W/m^2 in January and February to as much as 20 W/m^2 in May, evaluated at 86S latitude. In May the surface air temperature is only 234 K, so if the ERBE observations can be trusted, they do indicate that substantial cloud longwave forcing can occur even at low temperatures, and that the values can exceed the tropical values seen in the snowball simulation. On the other hand, the fact that there is negligible cloud forcing in January, when the temperature is considerably warmer, underscores the complexity of the processes determining cloud forcing.

[63] One can also attempt to compare observations of cloud water content with values predicted by the parameterization. Ground-based observations in the Antarctic by *Mahesh et al.* [2001a, 2001b] indicate winter and spring cloud base height of 1–3 km (apart from boundary layer clouds), and total cloud water content of .5–20 g/m^2. The control case cloud parameterization yields tropical cloud water path of 1.4 g/m^2 based on a cloud base height of 1.5 km: decidedly on the low end of the observed Antarctic range. On the other hand, the thick cloud case yields a cloud water path of 591 g/m^2, which vastly exceeds the observed range. Thus Antarctic clouds are thin and low, perhaps not so thin and low as the tropical clouds in the control snowball simulation, but certainly not so thick as those in the thick cloud experiment. We have not located any in situ aircraft observations of cloud water content over Antarctica, but some additional insight can nonetheless be drawn from observations of tropical and midlatitude clouds. In the present tropics, intense convection can loft a great deal of condensed water, leading to high cloud water content in the vicinity of convection. *McFarquhar and Heymsfield* [1996] report tropical anvil ice water content as high as 100 mg/m^3 at 10 km, falling to 5 mg/m^3 at 13 km. Midlatitude cirrus typically have lower water content, on the order of 10 mg/m^3 at 7 km [*Noone et al.*, 1991]. The prime significance of these numbers is in comparison to the thick cloud simulation. The thick cloud simulation has 20 mg/m^3 of cloud water at 10 km, but more importantly still has 8 mg/m^3 at 13 km, thus allowing optically thick clouds to penetrate to even greater altitudes than is the case for the modern hot tropics. This supports our contention that the thick cloud simulation greatly overestimates the likely cloud effect in the snowball regime. It is interesting to note that the control case parameterization underestimates the observed cloud water content when applied to the modern tropical climate, even though it has been tuned to yield approximately the correct cloud longwave forcing. For the modern tropics, the control case parameterization has only 5 mg/m^3 of cloud water at 10 km altitude but the underestimate of cloud optical thickness is made up for by the the fact that the GCM creates clouds that are more spread out in the horizontal and vertical than is the case in reality. This remark points up both the difficulty of comparing parameterized and observed clouds, and the essential difficulty of representing spatially intermittent clouds at the coarse scale of a GCM. The latter difficulty is common to all GCMs.

[64] Based on the above considerations, it seems quite possible that the parameterized cloud water in the control case significantly underestimates the cloud greenhouse effect, but the true value is unlikely to be as large as that in the thick cloud experiment. Since the latter does not achieve deglaciation, one can be moderately confident that more sophisticated cloud parameterizations would not in and of themselves provide a route to deglaciation.

8. Conclusions

[65] The aggregate effect of all the physics represented in the GCM but left out of prior deglaciation studies is to leave the annual mean equatorial ice surface temperature at a frigid 244 K even with .2 bars of CO_2 in the atmosphere. This is nearly 30 K short of the temperature where deglaciation is likely to commence, and the cold temperatures prevail despite a conservative choice of surface albedo parameters which are arguably unrealistically favorable to deglaciation. The principle ingredients maintaining such a cold climate are as follows: (1) The weak lapse rate occasioned by absence of convection in the winter hemisphere, (2) the strong seasonal cycle, which permits a considerable heat export from the tropics to the winter hemisphere, (3) extensive snow cover, increasing surface albedo, (4) reduction of ice surface temperature by a strong diurnal cycle rectified by nonlinearities in bulk surface heat fluxes, and (5) weak cloud greenhouse effects. These results are pertinent also to the general problem of recovery of the Early Earth or extrasolar planets from a frozen "cold start." If it is so hard to deglaciate Earth under Neoproterozoic conditions, it will be correspondingly harder at times of a yet fainter Sun; CO_2 clouds and buildup of alternate greenhouse gases become even more crucial to the recovery than previously thought.

[66] All of the phenomena inhibiting deglaciation are to some extent affected by parameterization, and it should be recognized that our simulation represents only the first step in the long process of coming to an understanding of the collective behavior of the climate system in fully glaciated conditions. Surface albedo and clouds offer many possibilities for surprises. The albedo of ice and snow is affected by

dust, bubble formation, and the complex physical structure of sea ice; we did not model any of these features, but did probe some of the sensitivity of the system. We found that fairly substantial reductions in the assumed ice albedo had little effect, because most of the ice is shielded by snow cover. Dark ice in conjunction with reduced snow cover, or dark, dusty snow, did produce a very substantial warming of the summertime maximum temperature, but much less increase in the equatorial annual mean temperature. The results are summarized in Table 3. Clouds are notoriously difficult to model, and in light of the primitive empirical cloud formulation used in our simulations, the predicted cloud forcing should be regarded as somewhat speculative. The parameterization yields thin, low clouds. Despite the cold climate, this result is not inevitable, since the moisture content of the low level atmosphere in the summer hemisphere would be sufficient to produce an optically thick cloud, if only it could be lofted and kept in suspension in the form of ice crystals. Thin clouds are nonetheless plausible, since making thicker clouds requires that convective updrafts be able to loft ice crystals faster than they fall, and this is not easy with the weak convection likely to prevail in the cold climate. Also, the large scale dynamical influences restricting cloud cover operate regardless of the cloud parameterization. Further progress on the problem of snowball Earth clouds will require cloud-resolving simulations in the cold convective regime, but in the meantime we probed the limits of cloud warming effects by performing an extreme experiment in which the cloud water content was forced to be comparable to that of modern tropical clouds. As for the experiments with reduced surface albedo, this produced a substantial increase of the summer maximum temperature, but much less increase in the maximum annual-mean ice surface temperature; transient daytime summer melt pools could occur in this simulation, but the temperature does not support sustained melting of the ice.

[67] The suppression of winter midlatitude convection, and the low summer tropopause, are not simple consequences of local radiative-convective considerations. These phenomena are affected in subtle ways by large scale dynamics and by boundary layer physics. The diurnal cycle is greatly enhanced by strong nocturnal cooling of the surface layers, which delays the onset of convection after the Sun rises. The strong nocturnal cooling is in turn caused by the inhibition of turbulent heat transfer through the stable boundary layer, but parameterization of turbulence in stable boundary layers constitutes one of the more challenging problems in atmospheric modeling.

[68] The strong diurnal cycle has several other important consequences. Through transient daytime melting, passage across the eutectic threshold and the diurnal precipitation-evaporation cycle it can affect the albedo of the surface, particularly once dust is brought into the picture. It supports the hypothesis that tropical sand wedges can form without the need for high obliquity. The nocturnal cooling lowers the daily average ice temperature, and inhibits deglaciation. Finally, transient noontime melting at the foot of glaciers adjacent to bare land could feed tropical ice-covered lakes and provide freshwater refugia for photosynthetic life.

[69] As on Mars, midlatitude storm tracks are primarily a winter phenomenon. The transient eddies that develop at the edge of the winter subtropics draw energy out of the tropics at a rate of about 2 Petawatts. While this is considerably less than the heat export in the modern climate, it is still sufficient to produce substantial tropical cooling because the reflective global ice surface greatly reduces the radiative driving of the climate system. Heat transport is consistently in the direction predicted by diffusion models, but the diagnosed diffusivity is lower than that commonly used in EBMs tuned to modern conditions. This is one of the few aspects of the GCM simulation that is more favorable to deglaciation than the corresponding EBM behavior. Part but not all of the reduced transport is thermodynamic, arising from the paucity of latent heat transport in the cold hard snowball climate. The diagnosed diffusivity is highly variable and does not appear to be related to the meridional temperature gradient in any simple way. This underscores the need for more sophisticated representations of midlatitude heat transport in simplified models.

[70] Somewhat surprisingly, there is a vigorous Hadley circulation in the tropics of the hard snowball, which is actually somewhat stronger than that of the much warmer modern climate. This circulation is very important to the deglaciation results, as it permits the cold winter subtropics to drag down the temperature of the entire tropics, and particularly the equatorial regions where the maximum annual average temperatures occur. In contrast with the modern Hadley circulation, the snowball Hadley circulation is unable to equalize free tropospheric temperatures across the tropics, and leaves the subsiding winter subtropical region with considerably higher static stability than that of the summer subtropics, which is nearly zero. The dynamics of this circulation raises many deep questions, which will be treated in a future paper.

[71] Could further increases of CO_2 lead to deglaciation? With our GCM it is not safe to increase the CO_2 much beyond .2 bars, since various neglected physical phenomena (detailed below) become progressively more important. However, an extrapolation from the present results provides some indication of the answer provided no additional physics enters the problem to substantially enhance the climate sensitivity. This is a questionable assumption, and we would not want to put undue emphasis on the results of extrapolation. For what it is worth, assuming each further doubling of CO_2 beyond .2 bars increases annual mean surface temperature by 3 K, a sensitivity somewhat greater than than simulated between .1 bars and .2 bars, we would conclude that the maximum temperature rises to only 253 K at 1.6 bars and 256 K at 3.2 bars. The implication is that one requires a very substantial enhancement of sensitivity to deglaciate even at these very elevated values.

[72] Assuming present outgassing rates [*Zhang and Zindler*, 1993] and assuming 2/3 of outgassed CO_2 goes into the ocean [*Higgins and Schrag*, 2003], it would already take 28 million years for .2 bar to accumulate in the atmosphere. There are considerable uncertainties in this estimate, particularly concerning the outgassing rate and the supply of carbonate. The latter is important because it ultimately determines the partitioning of CO_2 between the atmosphere and ocean. Reduced carbonate supply, as has been posited by *Ridgwell et al.* [2003], would allow more of the outgassed CO_2 to remain in the atmosphere, and the effect should become more pronounced as atmospheric CO_2 is increased beyond .2 bars and more of the marine

carbonate supply is exhausted. While it is clearly wrong to say that it would be impossible to build up 1 or 2 bars of CO_2 in the time available, it is fair to say that to do so pushes the limits of what is conceivable. A bigger concern with the hypothesis of extremely high CO_2 as a route to deglaciation is the effect of such high concentrations on the postglacial world, and the compatibility of the resulting extremely hot climate with available geochemical and physical evidence. This problem remains to be addressed.

[73] The GCM simulations we have discussed accurately incorporate the radiative effect of high CO_2, but there are certain thermodynamic and dynamic effects that have been neglected. Incorporating these in a standard terrestrial model poses formidable challenges requiring rewriting of virtually every line of the physics package. While the neglected effects are still quite weak at .2 bars, they become progressively more important with further increases of CO_2. One such effect concerns the lapse rate to which convection adjusts the temperature profile. At cold temperatures, the dry and moist adiabats are virtually identical, with the formula for the former in pressure coordinates being $T(p) = T(p_o)\,(p/p_o)^{R/C_p}$, where R and C_p are the gas constant and specific heat for the mixture of gases that makes up the atmosphere. For reasons grounded in statistical thermodynamics, R/C_p is determined primarily by molecular structure. Since N_2 and O_2 are both diatomic, their relative mixing ratios have little effect on R/C_p. A pure N_2 atmosphere would have $R/C_p = .2844$ while a pure O_2 atmosphere would have $R/C_p = .2827$ and both are close to the theoretical value of $\frac{2}{7}$ for diatomic molecules. CO_2 is triatomic, and has R/C_p in the range .22 to .23 near 1 bar and 273 K, with weak temperature and pressure dependance. A pure CO_2 atmosphere would thus have a weaker lapse rate (and weaker greenhouse effect) than an N_2/O_2 atmosphere with trace amounts of CO_2. The effect is not pronounced,however. For a pure CO_2 atmosphere, the 600 mb temperature is only 6 K warmer than it would be for a pure N_2 atmosphere, based on a surface temperature of 250 K. For a 50-50 mixture of CO_2 and air, the effect would be even weaker.

[74] If the composition of the rest of the atmosphere were held fixed, addition of massive amounts of CO_2 would increase the atmospheric pressure and therefore increase the infrared opacity of all atmospheric greenhouse gases through collisional line broadening. This effect is neglected in the simulations reported above; at .2 bars the neglected effect would reduce OLR by only about 2 W/m^2 if oxygen partial pressure were set at its present value (less if the oxygen content of the atmosphere were lower in the Neoproterozoic). As the CO_2 concentration is made higher, the warming due to pressure broadening becomes progressively more important. However, the cooling due to Rayleigh scattering from CO_2 also becomes more important, offsetting some of the effect. The increase of surface pressure would have dynamical as well as radiative effects. All other things being equal, synoptic eddies would be able to transfer heat more rapidly, owing to the greater atmospheric heat capacity. The change in atmospheric mass could also have effects on the eddies and the Hadley circulation themselves, though the nature of the effect is hard to anticipate without dynamic simulations.

[75] Perhaps the most important effect of highly elevated CO_2 would be through the onset of CO_2 condensation and consequent formation of dry-ice clouds. If CO_2 frost accumulates on the ground, it can limit the amount of CO_2 the atmosphere can hold. CO_2 clouds, however, can potentially exert a powerful warming effect on the atmosphere, depending on how certain unresolved microphysical issues play out [*Forget and Pierrehumbert*, 1997; *Pierrehumbert and Erlick*, 1997; *Colaprete and Toon*, 2003]. Even at .2 bars, it becomes cold enough near the winter pole for some limited CO_2 condensation to occur near the ground. Such condensation becomes widespread at 1 or 2 bars.

[76] Apart from further elevation of CO_2, there may be other routes to deglaciation. Cloud microphysics in a cold climate may permit thicker clouds than present parameterizations predict, and unanticipated modes of convection could change the lapse rate or tropopause height. Other greenhouse gases, notably methane and N_2O may enter the picture. Little is known about the sea ice dynamical regime associated with sea glacier flow, and there may be possibilities for forming thin ice regions and leads associated with fracture zones, or in association with hydrothermal plumes. It would be the height of hubris to speak, based on GCM simulations, of "impossibility" in connection with the problem of exiting a Neoproterozoic hard snowball. Nature has surprised us with many "impossible" things, notably the Antarctic Ozone Hole, and given the many interacting pieces of the climate system, there are ample possibilities for further surprises. The most that can be said is that one must look beyond the standard scenario to provide an answer to the deglaciation problem. Unquestionably, the Neoproterozoic presents us with a remarkable confluence of bizarre behavior of climate indicators which are sensitive to global conditions: large ^{13}C excursions, tropical glacial deposits, cap carbonates, and banded iron formations. The unusual behavior seems to call for a truly unusual global climate, and the hard snowball seems to fit the bill, whereas proposed cold climates with open tropical water [*Hyde et al.*, 2000] are only an exaggerated form of the conventional Pleistocene glacial-interglacial cycles. "Soft snowball" states require only a modest buildup of carbon dioxide to deglaciate, owing to the continuous operation of ice-albedo feedback.

[77] A more obvious, though not necessarily more correct, view of our results would be to say that they point toward the necessity of explaining Neoproterozoic climate without invoking a hard snowball. Modeling results on the difficulty of initiating a hard snowball have been interpreted in this way, but are inconclusive, perhaps more so than our identification of the deglaciation difficulty. Studies with a fully coupled ocean-atmosphere GCM [*Poulsen et al.*, 2001] do indeed show that dynamic ocean heat transports present a powerful impediment to initiation; given the important role of a dynamic ocean, earlier simulations on the difficulty of initiation [*Chandler and Sohl*, 2000; *Hyde et al.*, 2000] are hard to interpret, owing to their use of parameterized or specified ocean heat transports. Recently, it has been suggested that more accurate sea-ice physics could allow easier initiation despite ocean dynamic effects [*Donnadieu et al.*, 2004; *Lewis et al.*, 2003, 2004], though it should be noted that these ideas have not yet been tested in a model with both a fully dynamic atmosphere and ocean.

[78] A more pressing challenge to the hard snowball idea comes from the geological record. Evidence for active glaciers has sometimes been taken as incompatible with the sluggish hydrological cycle of a hard snowball [*Leather et al.*, 2002; *Kellerhals and Matter*, 2003], but it has been shown that even the feeble snowfall in a globally glaciated climate, accumulating over tens of thousands of years, can drive ice streams yielding active glacial features [*Donnadieu et al.*, 2003]. Evidence for open water in coastal regions [*Arnaud*, 2004] can perhaps be countered by the Snowball Oasis concept [*Halverson et al.*, 2004], which suggests that in late stages of a hard snowball open water in coastal regions can coexist with widespread tropical ice cover, owing to flow of sea glaciers. The interpretation of cap carbonates as being deposited in the aftermath of a hard snowball has also been questioned, on the grounds that they are not always associated with glacial deposits [*Lorentz et al.*, 2004], or that they show the wrong chemical weathering signature [*Kennedy et al.*, 2001b; *Young*, 2002; *James et al.*, 2001]. However, cap carbonates can form for a long time after deglaciation, and in places which are not propitious for accumulating glacial deposits. Moreover, the dissolution of carbonate can eliminate much of the expected imprint of weathering [*Higgins and Schrag*, 2003]. On the other hand, paleomagnetic data appearing to indicate that certain cap carbonates were laid down over a time spanning many geomagnetic reversals [*Trinidade et al.*, 2003] are highly problematic for the hard snowball hypothesis, and it remains to be seen whether an alternate interpretation of these results emerges. It has also been suggested that Neoproterozoic Banded Iron Formations (a general signature of oxygen-starved conditions) are more compatible with hydrothermal activity in rift basins than with a hard snowball [*Young*, 2002]. However, evidence of volcanic or hydrothermal activity is absent in many of the formations, and the hard snowball provides an explanation for the required low oceanic sulfate, whereas the rift mechanism does not. Global glaciation should leave some imprint on biology, and the lack of such evidence has sometimes been used to argue against a hard snowball. In particular, *Corsetti et al.* [2003] show continuity of biota across a putative snowball boundary. It is possible that this puzzling result is an artifact due to windborne redistribution of microfossils stranded on land (P. Hoffman, personal communication). Sulfur isotope perturbations do give an indication of massive reorganization of marine biochemistry [*Hurtgen et al.*, 2002]; this finding has been questioned by *Shields et al.* [2004], but the deposits discussed there are all in fact postsnowball age, and moreover the earlier glacial-era results have now been replicated in other Neoproterozoic deposits [*Hurtgen et al.*, 2005]. The support for the hard snowball found in the geological record may be equivocal, but there is nothing in the record which clearly knocks the hard snowball out of the running.

[79] Among alternate attempts to explain the mysterious features of Neoproterozoic climate, the proposal of a wholly stagnant, stratified open ocean is highly implausible (as per arguments summarized in *Hoffman and Schrag* [2002]), and the proposal of high obliquity [*Williams et al.*, 1998] has been almost definitively discarded [*Donnadieu et al.*, 2002; *Ramstein et al.*, 2004; *Levrard and Laskar*, 2003]. Additional theories may ultimately emerge but for now the one alternate theory remaining in play invokes a severe ice age leaving open tropical oceans, followed by massive releases of methane from destabilized marine clathrates [*Kennedy et al.*, 2001a, 2001b]. Some objections to this theory are given in *Hoffman and Schrag* [2002]. Some of these objections are addressed in *Jiang et al.* [2003], which presents geochemical evidence for the existence of Neoproterozoic methane seeps. The idea of a clathrate-based explanation for Neoproterozoic climate is undoubtedly a very interesting one, but its consequences need to be elaborated theoretically before it can be given a fair test. Can the required amount of methane be released, and on a suitable timescale? What kind of ocean circulation would provoke the release? Does the methane reach the atmosphere already oxidized in the ocean, or as methane gas, and if the latter, what is its lifetime in the atmosphere (a question requiring modeling of atmospheric chemistry)? Is there enough sulfate in the Neoproterozoic ocean to allow the needed anaerobic oxidation of the methane [see *Kah et al.*, 2005; *Hurtgen et al.*, 2002]? What are the climate impacts of the methane release, and what are the consequences of the attendant precipitation changes for weathering and the time-course of atmospheric CO_2? The question of whether the clathrate hypothesis is supported by the geological record cannot be adequately addressed without more climate and geochemical modeling of this sort. It is an interesting endeavor, which has been rather neglected in comparison with the hard snowball hypothesis.

[80] While the hard snowball hypothesis cannot by any stretch of the imagination be said to find the same degree of support in theory and the geological record as plate tectonics, neither can it be said to have been clearly displaced by any competing explanation of Neoproterozoic climate. The passage through a Neoproterozoic hard snowball state would be so remarkably interesting, if true, that it repays further study even though some might assign a low probability to such an event having actually happened. The continued quest for a viable route to deglaciation will no doubt lead to many new insights about the operation of the climate system.

[81] **Acknowledgments.** In carrying out this work, I had the benefit of many illuminating discussions with Paul Hoffman and Steve Warren. Ken Caldeira and Jim Kasting provided some much needed assistance in sorting out some details regarding predictions of EBM simulations. Rob Jacob's indispensible advice on working with FOAM is also gratefully acknowledged. Extensive conversations with Gilles Ramstein helped me to appreciate the extent to which the GCM results could depend on parameterization assumptions, and an anonymous reviewer helped me to appreciate a broader spectrum of the geological and geochemical literature on the Neoproterozoic. I thank the Laboratoire de Meteorologie Dynamique, Paris, for providing a congenial environment for bringing the project to fruition. This work is a contribution of the University of Chicago Climate Systems Center, funded by the National Science Foundation under grants ATM-0121028 and ATM-0123999.

References

Arnaud, E. (2004), Giant cross-beds in the Neoproterozoic Port Askaig Formation, Scotland: Implications for snowball Earth, *Sediment. Geol.*, *165*(1–2), 155–174.

Barry, L. J., G. C. Craig, and J. Thuburn (2002), Poleward transport by the atmospheric heat engine, *Nature*, *415*, 774–777.

Caldeira, K., and J. F. Kasting (1992), Susceptibility of the early Earth to irreversible glaciation caused bycarbon dioxide clouds, *Nature*, *359*, 226–228.

Chandler, M. A., and L. E. Sohl (2000), Climate forcings and the initiation of low-latitude ice sheets during the Neoproterozoic Varanger glacial interval, *J. Geophys. Res.*, *105*(D16), 20,737–20,756.

Colaprete, A., and O. B. Toon (2003), Carbon dioxide clouds in an early dense Martian atmosphere, *J. Geophys. Res.*, *108*(E4), 5025, doi:10.1029/2002JE001967.

Collins, M., et al. (1996), Baroclinic wave transitions in the Martian atmosphere, *Icarus*, *120*(2), 344–357.

Corsetti, F. A., S. M. Awramik, and D. Pierce (2003), A complex microbiota from snowball Earth times: Microfossils from the Neoproterozoic Kingston Peak Formation, Death Valley, USA, *Proc. Natl. Acad. Sci. U. S. A.*, *100*(8), 4399–4404.

Donnadieu, Y., et al. (2002), Is high obliquity a plausible cause for Neoproterozoic glaciations?, *Geophys. Res. Lett.*, *29*(23), 2127, doi:10.1029/2002GL015902.

Donnadieu, Y., F. Fluteau, G. Ramstein, C. Ritz, and J. Besse (2003), Is there a conflict between the Neoproterozoic glacial deposits and the snowball Earth interpretation: An improved understanding with numerical modeling, *Earth Planet. Sci. Lett.*, *208*, 101–112.

Donnadieu, Y., et al. (2004), The impact of atmospheric and oceanic heat transports on the sea-ice-albedo instability during the Neoproterozoic, *Clim. Dyn.*, *22*(2–3), 293–306.

Forget, F., and R. T. Pierrehumbert (1997), Warming early Mars with carbon dioxide clouds that scatter infrared radiation, *Science*, *278*, 1273–1276.

Goodman, J. C., and R. T. Pierrehumbert (2003), Glacial flow of floating marine ice in snowball Earth, *J. Geophys. Res.*, *108*(C10), 3308, doi:10.1029/2002JC001471.

Halverson, G. P., A. C. Maloof, and P. F. Hoffman (2004), The Marinoan glaciation (Neoproterozoic) in northeast Svalbard, *Basin Res.*, *16*(3), 297–324.

Hanel, R. A., et al. (1972), Nimbus 4 Infrared Spectroscopy Experiment: 1. Calibrated thermal emission-spectra, *J. Geophys. Res.*, *77*, 2629–2641.

Held, I. M. (1978), The vertical scale of an unstable baroclinic wave and its importance for eddy heat flux parameterisation, *J. Atmos. Sci.*, *35*, 572–576.

Held, I. M., and A. Y. Hou (1980), Nonlinear axially symmetric circulations in a nearly inviscid atmosphere, *J. Atmos. Sci.*, *37*, 515–533.

Held, I. M., and V. D. Larichev (1996), A scaling theory for horizontally homogeneous, baroclinically unstable flow on a beta plane, *J. Atmos. Sci.*, *53*, 946–952.

Held, I. M., and B. J. Soden (2000), Water vapor feedback and global warming, *Annu. Rev. Energy Environ.*, *25*, 441–475.

Higgins, J. A., and D. P. Schrag (2003), Aftermath of a snowball Earth, *Geochem. Geophys. Geosyst.*, *4*, doi:10.1029/2002GC000403.

Hoffman, P. F., and D. P. Schrag (2002), The snowball Earth hypothesis: Testing the limits of global change, *Terra Nova*, *14*, 129–155.

Hoffman, P. F., A. J. Kaufman, G. P. Halverson, and D. P. Schrag (1998), A Neoproterozoic snowball Earth, *Science*, *281*, 1342–1346.

Hurtgen, M. T., M. A. Arthur, N. S. Suits, and A. J. Kaufman (2002), The sulfur isotopic composition of Neoproterozoic seawater sulfate: Implications for a snowball Earth?, *Earth Planet. Sci. Lett.*, *203*, 413–429.

Hurtgen, M. T., M. A. Arthur, and G. P. Halverson (2005), Neoproterozoic S isotopes, the evolution of microbial S species, and the burial efficiency of sulfide as sedimentary pyrite, *Geology*, in press.

Hyde, W. T., T. J. Crowley, S. K. Baum, and W. R. Peltier (2000), Neoproterozoic "snowball Earth" simulations with a coupled climate/ice-sheet model, *Nature*, *405*, 425–429.

Ikeda, T., and E. Tajika (1999), A study of the energy balance climate model with CO_2-dependent outgoing radiation: Implication for the glaciation during the Cenozoic, *Geophys. Res. Lett.*, *26*, 349–352.

Intergovernmental Panel on Climate Change (IPCC) (2001), *Climate Change 2001: The Scientific Basis—Contribution of Working Group I to the Third Assessment Report of the Intergovernmental Panel on Climate Change*, edited by J. T. Houghton et al., 881 pp., Cambridge Univ. Press, New York.

Jacob, R. (1997), Low frequency variability in a simulated atmosphere ocean system, Ph.D. thesis, 159 pp., Univ. of Wis., Madison.

James, N. P., G. M. Narbonne, and T. K. Kyser (2001), Late Neoproterozoic cap carbonates: Mackenzie Mountains, northwestern Canada: Precipitation and global glacial meltdown, *Can. J. Earth Sci.*, *38*(8), 1229–1262.

Jenkins, G. S. (2003), GCM greenhouse and high-obliquity solutions for early Proterozoic glaciation and middle Proterozoic warmth, *J. Geophys. Res.*, *108*(D3), 4118, doi:10.1029/2001JD001582.

Jiang, G., M. J. Kennedy, and N. Christie-Blick (2003), Stable isotopic evidence for methane seeps in Neoproterozoic postglacial cap carbonates, *Nature*, *426*(6968), 822–826.

Kah, L. C., T. W. Lyons, and T. D. Frank (2005), Low marine sulphate and protracted oxygenation of the Proterozoic biosphere, *Nature*, doi:10.1038/nature02974, in press.

Kalnay, E., et al. (1996), The NCEP/NCAR 40-Year Reanalysis Project, *Bull. Am. Meteorol. Soc.*, *77*, 437–471.

Kasting, J. F., and T. P. Ackerman (1986), Climatic consequences of very high carbon dioxide levels in the Earth's early atmosphere, *Science*, *234*(4782), 1383–1385.

Kellerhals, P., and A. Matter (2003), Facies analysis of a glaciomarine sequence, the Neoproterozoic Mirbat Sandstone Formation, Sultanate of Oman, *Eclogae Geol. Helv.*, *96*(1), 49–70.

Kennedy, M. J., N. Christie-Blick, and L. E. Sohl (2001a), Are Proterozoic cap carbonates and isotopic excursions a record of gas hydrate destabilization following Earth's coldest intervals?, *Geology*, *29*(5), 443–446.

Kennedy, M. J., N. Christie-Blick, and A. R. Prave (2001b), Carbon isotopic composition of Neoproterozoic glacial carbonates as a test of paleoceanographic models for snowball Earth phenomena, *Geology*, *29*(12), 1135–1138.

Kiehl, J. T., J. J. Hack, G. B. Bonan, B. A. Boville, D. L. Williamson, and P. J. Rasch (1998), The National Center for Atmospheric Research Community Climate Model: CCM3, *J. Clim.*, *11*, 1131–1149.

Kirschvink, J. L. (1992), Late Proterozoic low-latitude global glaciation: The snowball Earth, in *The Proterozoic Biosphere*, edited by J. W. Schopf and C. Klein, p. 5152, Cambridge Univ. Press, New York.

Leather, J., P. A. Allen, M. D. Brasier, and A. Cozzi (2002), Neoproterozoic snowball Earth under scrutiny: Evidence from the Fiq glaciation of Oman, *Geology*, *30*(10), 891–894.

Levrard, B., and J. Laskar (2003), Climate friction and the Earth's obliquity, *Geophys. J. Int.*, *154*(3), 970–990.

Lewis, J. P., et al. (2003), Neoproterozoic "snowball Earth": Dynamic sea ice over a quiescent ocean, *Paleoceanography*, *18*(4), 1092, doi:10.1029/2003PA000926.

Lewis, J. P., et al. (2004), Global glaciation in the Neoproterozoic: Reconciling previous modeling results, *Geophys. Res. Lett.*, *31*, L08201, doi:10.1029/2004GL019725.

Lindzen, R. S., and A. Y. Hou (1988), Hadley circulations for zonally averaged heating centered off the equator, *J. Atmos. Sci.*, *45*, 2416–2427.

Lorentz, N. J., F. A. Corsetti, and P. K. Link (2004), Seafloor precipitates and C-isotope stratigraphy from the Neoproterozoic Scout Mountain Member of the Pocatello Formation, southeast Idaho: Implications for Neoproterozoic Earth system behavior, *Precambrian Res.*, *130*(1–4), 57–70.

Mahesh, A., V. P. Walden, and S. G. Warren (2001a), Ground-based infrared remote sensing of cloud properties over the Antarctic Plateau. part I: Cloud base heights sizes, *J. Appl. Meteorol.*, *40*, 1265–1278.

Mahesh, A., V. P. Walden, and S. G. Warren (2001b), Ground-based infrared remote sensing of cloud properties over the Antarctic Plateau. part II: Cloud optical depths and particle sizes, *J. Appl. Meteorol.*, *40*, 1279–1294.

Maloof, A. C., J. B. Kellogg, and A. M. Anders (2002), Neoproterozoic sand wedges: Crack formation in frozen soils under diurnal forcing during a snowball Earth, *Earth Planet. Sci. Lett.*, *204*, 1–15.

McFarquhar, G. M., and A. J. Heymsfield (1996), Microphysical characteristics of three anvils sampled during the Central Equatorial Pacific Experiment, *J. Atmos. Sci.*, *53*, 2401–2423.

Noone, K. B., K. J. Noone, J. Heintzenberg, J. Strom, and J. A. Ogren (1991), In situ observations of cirrus cloud microphysical properties using the counterflow virtual impactor, *J. Atmos. Oceanic Technol.*, *10*, 294–303.

Pierrehumbert, R. T. (1995), Thermostats, radiator fins, and the local runaway greenhouse, *J. Atmos. Sci.*, *52*, 1784–1806.

Pierrehumbert, R. T. (2002), The hydrologic cycle in deep-time climate problems, *Nature*, *419*, 191–198.

Pierrehumbert, R. T. (2004), High levels of atmospheric carbon dioxide necessary for the termination of global glaciation, *Nature*, *429*, 646–649.

Pierrehumbert, R. T., and C. Erlick (1997), On the scattering greenhouse effect of CO_2 ice clouds, *J. Atmos. Sci.*, *55*, 1897–1903.

Pierrehumbert, R. T., and K. L. Swanson (1995), Baroclinic instability, *Ann. Rev. Fluid Mech.*, *27*, 419–467.

Poulsen, C., R. T. Pierrehumbert, and R. Jacob (2001), Impact of ocean dynamics on the simulation of the Neoproterozoic "snowball Earth," *Geophys. Res. Lett.*, *28*, 1575–1578.

Ramanathan, V., R. D. Cess, E. F. Harrison, P. Minnis, B. R. Barkstrom, E. Ahmad, and D. Hartman (1989), Cloud-radiative forcing and the climate: Results from the Earth Radiation Budget Experiment, *Science*, *243*, 57–63.

Ramstein, G., Y. Donnadieu, and Y. Godderis (2004), Proterozoic glaciations, *Comptes Rendus Geosci.*, *336*(7–8), 639–646.

Ridgwell, A. J., M. J. Kennedy, and K. Caldeira (2003), Carbonate deposition, climate stability, and Neoproterozoic ice ages, *Science*, *302*, 859–862.

Schneider, T. (2005), The tropopause and the thermal stratification of the extratropics of a dry atmosphere, *J. Atmos. Sci.*, in press.

Semtner, A. J. (1976), A model for the thermodynamic growth of sea ice in numerical investigations of climate, *J. Atmos. Sci.*, *6*, 379–389.

Shields, G., H. Kimura, J. D. Yang, and P. Gammon (2004), Sulphur isotopic evolution of neoproterozole-Cambrian seawater: New francolite-bound sulphate delta S-34 data and a critical appraisal of the existing record, *Chem. Geol.*, *204*(1–2), 163–182.

Tajika, E. (2003), Faint young Sun and the carbon cycle: Implication for the Proterozoic global glaciations, *Earth Planet. Sci. Lett.*, *214*, 443–453.

Trenberth, K. E., and J. M. Caron (2001), Estimates of meridional atmosphere and ocean heat transports, *J. Clim.*, *14*, 3433–3443.

Trinidade, R. I. F., E. Font, M. S. D'Agrella, A. C. R. Nogueira, and C. Riccomini (2003), Low-latitude and multiple geomagnetic reversals in the Neoproterozoic Puga cap carbonate, Amazon craton, *Terra Nova*, *15*(6), 441–446.

Walker, J. C. G. (2001), Strange weather on snowball Earth, in *Proceedings of Conference on Earth System Processes, Edinburgh, Scotland*, p. 110–111, Geol. Soc., London.

Warren, S. G., R. E. Brandt, T. C. Grenfell, and C. P. McKay (2002), Snowball Earth: Ice thickness on the tropical ocean, *J. Geophys. Res.*, *107*(C10), 3167, doi:10.1029/2001JC001123.

Williams, D. M., J. F. Kasting, and L. A. Frakes (1998), Low-latitude glaciation and rapid changes in the Earth's obliquity explained by obliquity-oblateness feedback, *Nature*, *396*, 453–455.

Young, G. M. (2002), Stratigraphic and tectonic settings of Proterozoic glaciogenic rocks and banded iron-formations: Relevance to the snowball Earth debate, *J. Afr. Earth Sci.*, *35*(4), 451–466.

Zhang, Y. X., and A. Zindler (1993), Distribution and evolution of carbon and nitrogen in Earth, *Earth Planet. Sci. Lett.*, *117*, 331–345.

R. T. Pierrehumbert, Department of Geophysical Sciences, University of Chicago, Chicago, IL 60637, USA. (rtp1@geosci.uchicago.edu)